INVESTIGATION OF THE ROLE OF GLYPICAN 3 IN LIVER REGENERATION AND HEPATOCYTE PROLIFERATION

By

BOWEN LIU

B.S. in Biological Science and Technology,

Tsinghua University, Beijing China, 2005

Submitted to the Graduate Faculty of the

University of Pittsburgh School of Medicine,

Division of Cellular and Molecular Pathology

Department of Pathology

in partial fulfillment of the requirements for the degree of

Doctor of Philosophy

University of Pittsburgh

2010

UNIVERSITY OF PITTSBURGH

School of Medicine

This dissertation was presented

by

BOWEN LIU

It was defended on

August 13, 2010

and approved by

Chuanyue Wu, Ph.D., Professor, Department of Pathology

Jian-hua Luo, Ph.D., Associate Professor, Department of Pathology

Satdarshan P. Singh Monga, Ph.D., Associate Professor, Department of Pathology

James L. Funderburgh, Ph.D., Associate Professor, Departments of Ophthalmology & Cell Biology & Physiology

Committee Chair: Wendy Mars, Ph.D., Associate Professor, Department of Pathology

Dissertation Advisor: George K. Michalopoulos, M.D., Ph.D., Professor and Chairman, Department of Pathology

INVESTIGATION OF THE ROLE OF GLYPICAN 3 IN LIVER REGENERATION AND HEPATOCYTE PROLIFERATION

Bowen Liu, Ph.D.

University of Pittsburgh, 2010

Glypican 3 (GPC3) belongs to a family of glycosylphosphatidylinositol-anchored, cell-surface heparan sulfate proteoglycans. The GPC3 gene is located on the X chromosome, and is highly expressed during embryogenesis and organogenesis. Loss-of-function mutations of GPC3 in humans result in the Simpson-Golabi-Behmel syndrome, an X-linked disorder characterized by pre- and post-natal liver and other organ overgrowth. GPC3 is one of the most over-expressed proteins in human hepatocellular carcinoma and is used as a novel diagnostic marker. However, its role in normal liver regeneration is still not well characterized. In this study, we investigated the role and effects of GPC3 in hepatocyte proliferation and liver regeneration, using the 2/3 partial hepatectomy (PHx) model in rats and hepatocyte-targeted GPC3 transgenic mice. We found in rats that GPC3 mRNA and protein increase in a time frame which coincides with the termination of proliferative activities of either hepatocytes (day 2 after PHx and day 8-12 in culture) or non-parenchymal cells (day 5-6 after PHx). Blocking GPC3 expression using morpholino oligonucleotides promoted rat hepatocyte growth *in vitro*. We further generated GPC3 transgenic mice with hepatocyte-targeted over-expression of GPC3. These transgenic mice develop normally compared with their non-transgenic littermates, but have a suppressed rate of hepatocyte proliferation and liver regeneration after 2/3 PHx. Therefore we hypothesize that GPC3 is a negative regulator of hepatocyte proliferation and liver regeneration. The yeast two-hybrid assay revealed that GPC3 interacts with several interesting proteins including CD81, a cell membrane tetraspanin. CD81 levels changed in the same manner as GPC3 after rat PHx, and their interaction was confirmed by co-immunoprecipitation and co-immunofluorescence. The co-localization of GPC3 and CD81 after PHx indicates an important regulator interaction between the two proteins. Moreover, gene array analysis revealed a series of changes in the expression profiles in GPC3 transgenic mice. After PHx, a panel of cell cycle related genes and

some oncogenes are either up- or down-regulated, which was confirmed by western blotting. Our results indicate that GPC3 plays a negative regulatory role in hepatocyte proliferation and liver regeneration in rats and hepatocyte-targeted transgenic mice, in which several potential proteins and multiple pathways are involved and affected.

TABLE OF CONTENTS

LIST OF TABLES

LIST OF FIGURES

LIST OF ABBREVIATIONS

Afm: afamin

AFP: alpha-fetoprotein

Afr2: Alpha-fetoprotein regulator 2

AP1: Activator protein 1

Ass: argininosuccinate synthetase

BMP: bone morphogenetic protein

CCl4: carbon tetrachloride

Catnb: beta catenin

Ccn: Cyclin

Ccnd1: Cyclin D1

C/EBP: CCAAT-enhancer-binding protein

Dbp: D site Albumin promoter binding

DEN: diethylnitroamine

DMSO: dimethyl sulfoxide

ECM: extracellular matrix

Egfr: epidermal growth factor receptor

Egr-1: early growth response factor 1 protein

ERK: extracellular signal-regulated kinase

Fgf14: fibroblast growth factor 14

Gabaar: GABA-A receptor

Gadd45b: growth arrest and DNA-damage-inducible 45 beta

Gas1: growth arrest specific 1

GAG: glycosaminoglycan

GPC3: glypican 3

GPCR: G protein-coupled receptor

GPI: glycosylphosphatidylinositol

HBGF: heparin-binding growth factor

HCC: hepatocellular carcinoma

HCV: hepatitis C virus

HGF: hepatocyte growth factor

HGM: hepatocyte growth medium

Hh: hedgehog

HNF1: hepatic nuclear factor 1

HS: heparan sulfate

HSPG: heparan sulfate proteoglycans

IGF2: insulin-like growth factor 2

Igfbp1: insulin-like growth factor binding protein 1

IL-6: interleukin 6

Jak3: Janus kinase 3

MAPK: mitogen activated protein kinase

MTA: multitumor array

Mthfs: 5,10-methenyltetrahydrofolate synthetase

Ndl: Nodal

NICD: Notch intracellular domain

NF-κB: nuclear factor kappa B

NPC: non-parenchymal cells

Oligos: oligonucleotides

PBGD: porphobilinogen deaminase

PBS: phosphate buffered saline

PLC: phospholipase C

PHx: partial hepatectomy

Poly A: polyadenylation

Ptgds: prostaglandin D2 synthase

Rab2: RAS oncogene family

RIPA: radioimmunoprecipitation assay

Rps2: ribosomal protein S2

Runx3: runt related transcription factor 3

SGBS: Simpson-Golabi-Behmel syndrome

STAT3: signal transducer and activator of transcription-3

SULF2: sulfatase 2

TBST: Tris-buffered saline Tween 20

TCA: trichloroacetic acid

TEM: tetraspanin-enriched microdomain

TG: transgenic

Tgfβ1: transforming growth factor beta type I

TGF-α: transforming growth factor-α

TNF-α: tumor necrosis factor-α

uPA: urokinase plasminogen activator

Wnt7b: wingless-related MMTV integration site 7B

WT: wild-type

YAP: yes-associated protein

Zhx2: zinc fingers and homeoboxes 2

PREFACE

I still remember the first time I stepped into Pittsburgh, five years ago, when I was wandering in the Oakland campus and struggling for a picture of myself as a Ph.D. With all the expectations of my new beginning along with a bit of fear from having to stand on my own in a completely different place, I not only managed to survive, but I was also able to live, to learn, to grow, and to enjoy the happiest and most fulfilling five years of my life.

This Ph.D. degree is not only a diploma that makes my family so proud, but an important witness of my experiences in academia and in life, overcoming all the difficulties to reach all the achievements that I did not always know I could achieve. I would have never been able to do it without the people who walked with me through all the good and the bad times. Therefore, I would like to take this opportunity to express my deep gratefulness to them.

First, I want to thank my advisor, **Dr. George Michalopoulos**, who has been my mentor not only in my dissertation projects, but also in my life. He led me into this fascinating world of scientific discovery, and directed me through the challenges whenever my experiments hit an obstacle. George relentlessly supported and encouraged me while never showing any signs of impatience or disappointment. I will never forget his precision and enthusiasm toward science, as well as his generous and optimistic attitude toward life. I can only hope to possess the same attributes someday in my future, and eventually become a person like him.

I would also like to thank my committee chair, **Dr. Wendy Mars**, for her generous help and valuable advice for my experiments as well as my career path. I also deeply appreciate the help and support from my committee: **Drs. Paul Monga**, **Jian-hua Luo**, **Cary Wu** and **James Funderburgh**. I received so many brilliant ideas and so much inspiration from them through our truly enjoyable discussions. I also want to acknowledge my fellow researchers and colleagues: **Mr. Bill Bowen**, **Dr. Shirish Paranjpe**, **Dr. Aaron Bell**, **Dr. Jaspal Khillan**, **Dr. Pallavi Limaye**, **Dr. Udayan Apte**, **Dr. Yu Yang**, **Jennifer Hurd**, **Ann Orr**, **Rachel Stewart**, **Liang-I Kang**, **Dr. Shashi Donthamsetty** and **Dr. Vishakha Bhave** for their assistance and guidance. It was such a wonderful pleasure to work with all of them and to share all the sweet memories.

Most importantly, I want to express my thankfulness and my love to **my parents**, who have given me so much support and strength to walk this far. Their unconditional love and trust will sustain me through any hurdles and challenges that I may face. In addition, I want to thank my beloved husband, **Yue Zhang**. We met, dated and happily married in Pittsburgh, all of which seemed so perfectly predestined. Always being so supportive, considerate and dedicated, he is the man to depend on through all my hard times, and the remainder of our lifetime.

Life's a journey, not a destination, and so is science. I feel blessed to have had such fantastic company on this journey. Thank you all again for accompanying me on my journey and letting me do the same for you.

With sincere respect and appreciation,

Bowen Liu

刘博闻

1.0 INTRODUCTION

1.1 GLYPICAN 3 (GPC3)

1.1.1 Glypicans

Glypicans (GPCs) are a family of heparan sulfate proteoglycans (HSPG) that are bound to the cell surface through a glycosylphosphatidylinositol (GPI) anchor (1). Six glypicans have been identified in mammals so far (GPC1 to GPC6) (Fig.1) (2) and two members of this family have been found in *Drosophila* (dally and dlp) (3). The mammalian glypican family members are further separated into two groups according to the degree of amino acid sequence homology (2). One group, which includes GPC1, GPC2, GPC4 and GPC6, displays 35–63% sequence similarity between its members. The other group is comprised of GPC3 and GPC5, which are 54% similar (2). The similarities between members of the two groups are only 17–25%.

Although the homology of amino acids between glypican members is moderate, the core proteins of all glypicans are approximately 500 amino acids in length and 60–70 kDa in size, and share a characteristic pattern of 14 conserved cysteine residues (Fig.1) (4). Discrepancies exist between

the predicted and observed molecular weights, owing to varying degrees of N- and/or O-glycosylations (2).

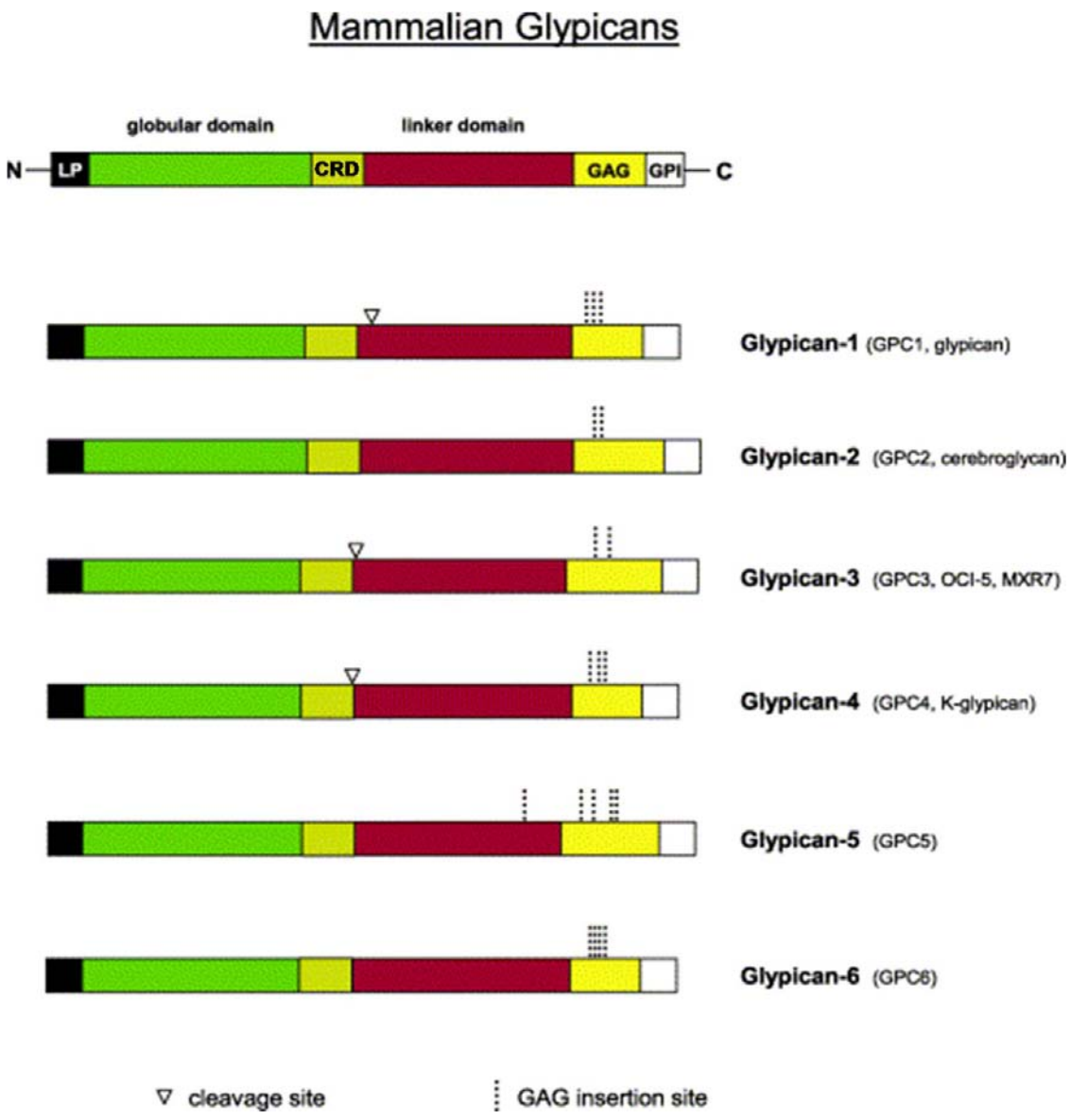

Figure 1. Mammalian Glypican Family Members. LP, leader peptide; CRD, cysteine-rich domain; GAG, glycosaminoglycan chains; GPI, glycosylphosphatidylinositol anchor. Reproduced from reference (2).

Intact glypicans are decorated with heparan sulfate (HS), which is located in the last 50 amino acids of the C-terminus, placing the HS chains close to the cell membrane (Fig.2) (5,6). This feature clearly distinguishes glypicans from syndecans, the other family of membrane-bound HSPGs, since in the syndecans the glycosaminoglycan (GAG) insertion sites can be found all along the core proteins (2). In addition to the GAG containing region, the mature glypican core proteins also have a linker domain and an N-terminal globular domain, with an internal proteolytic cleavage site identified at the proposed globular domain/linker junction (2). However, the 30-40 kDa cleavage product generated from the N-terminus of the glypican protein core remains attached to its C-terminal half through one or more disulfide bridges, and may be released into the extracellular environment under certain circumstance (2,7).

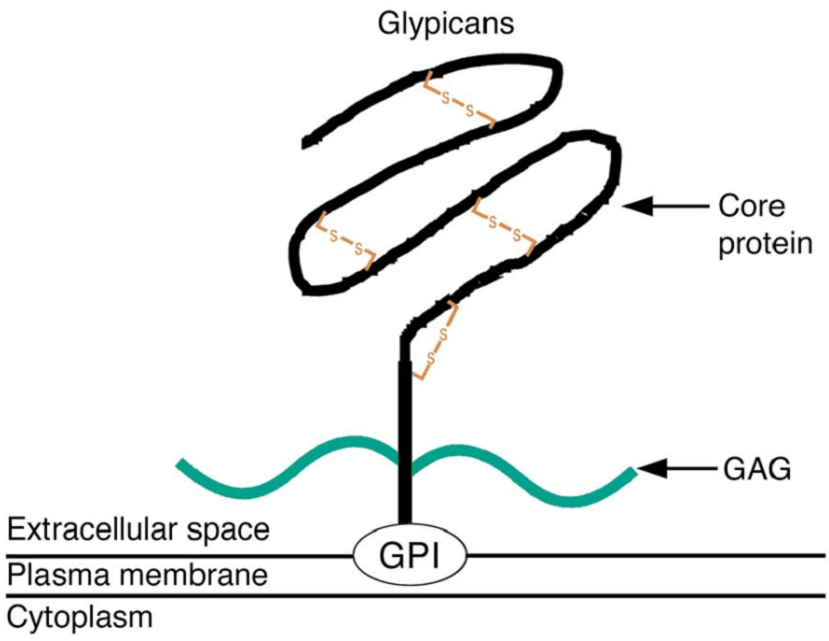

Figure 2. Schematic Diagram of Glypicans. GPI, glycosylphosphatidylinositol anchor; GAG, glycosaminoglycan chains. Reproduced from reference (6).

Glypicans are expressed predominantly during development (8). Their expression levels change in a stage- and tissue-specific manner, suggesting that glypicans are involved in the regulation of morphogenesis (7). The expression patterns and suggested roles among glypican family members varies greatly depending on the tissue or cellular context (2,7). The current understanding of the functions and mechanisms of mammalian glypicans mainly rests on the studies of glypican 3 (GPC3), the clinical significance of which has gained increasing attention and interest in the fields of morphogenesis and tumorigenesis.

1.1.2 GPC3 in Human Diseases

GPC3 is located at chromosome Xq26.1 and spans more than 500 kb (9,10), consisting of eight exons (11). High levels of GPC3 can be found in most tissues during embryogenesis and organogenesis, with the exception of the nervous system (2,7,12). In the adult, GPC3 can only be detected in a limited number of tissues, including the lung, ovaries, mammary epithelium, and mesothelium (2,13). The stage- and tissue- specific pattern of expression suggests that GPC3 is involved in morphogenesis and development.

It is reported that a loss-of -function mutation in the GPC3 gene causes Simpson-Golabi-Behmel syndrome (SGBS), an X-linked disorder characterized by pre- and post-natal overgrowth, increased risk of embryonic tumors during early childhood, and numerous visceral and skeletal anomalies (Fig.3) (12,14,15). It was found that SGBS is caused by a nonfunctional GPC3

protein, with additional genetic factors responsible for the intra- and interfamilial phenotypic variation (10,14). The involvement of GPC3 in SGBS was confirmed by the generation of GPC3-deficient mice (GPC3-/-), since these mice display some of the phenotypic features of SGBS, including developmental overgrowth (~ 30 %), and general enlargement of multiple organ including liver, respiratory infections, cystic kidneys, etc. (16).

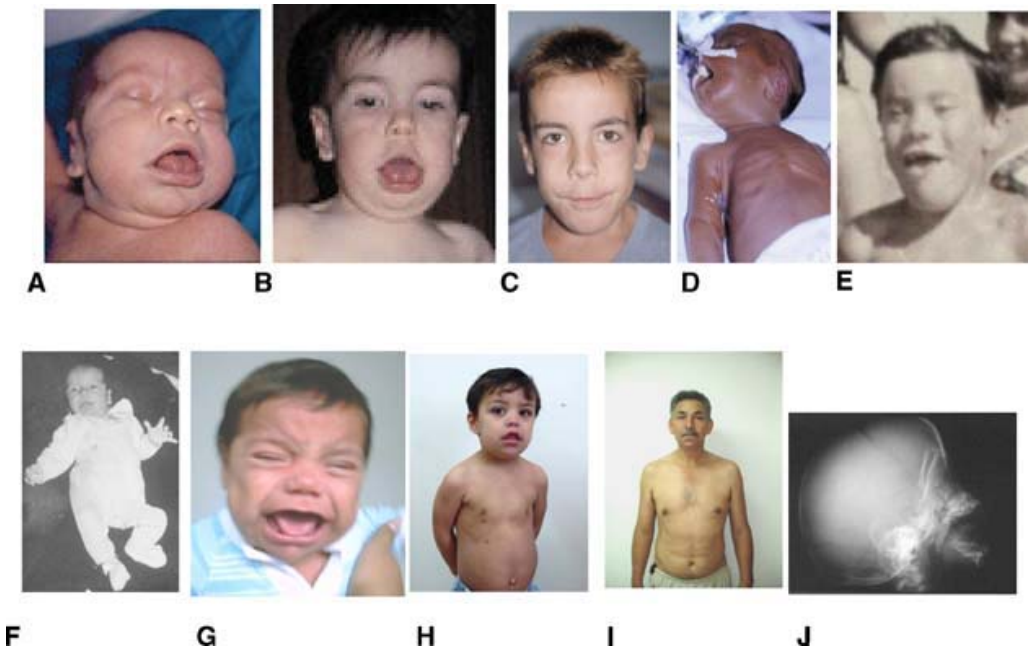

Figure 3. Typical Manifestations of Simpson-Golabi-Behmel Syndrome (SGBS). SGBS is characterized by pre- and post-natal macrosomia, characteristic facial anomalies and abnormalities affecting the internal organs, skeleton, and on some occasions, mental retardation of variable degree. Reproduced from reference (15).

One the other hand, GPC3 is highly up-regulated in hepatocellular carcinoma (HCC), one of the most common solid malignancies in the world that accounts for about 1 million deaths each year (17). Our previous study and others have shown that GPC3 is highly up-regulated in HCC and

hepatoblastoma, but not in normal liver or tissue adjacent to tumors (Fig.4) (17,18). In cancer cells, the mature form of GPC3 is processed by releasing the N-terminal truncated protein of 40 kDa into the medium (18). The soluble form of GPC3 was identified in the serum of patients with hepatocellular carcinomas, and can be used as a serological test for the diagnosis of HCC (18-20). GPC3 is also involved in cell proliferation in some hepatoma cell lines (21).

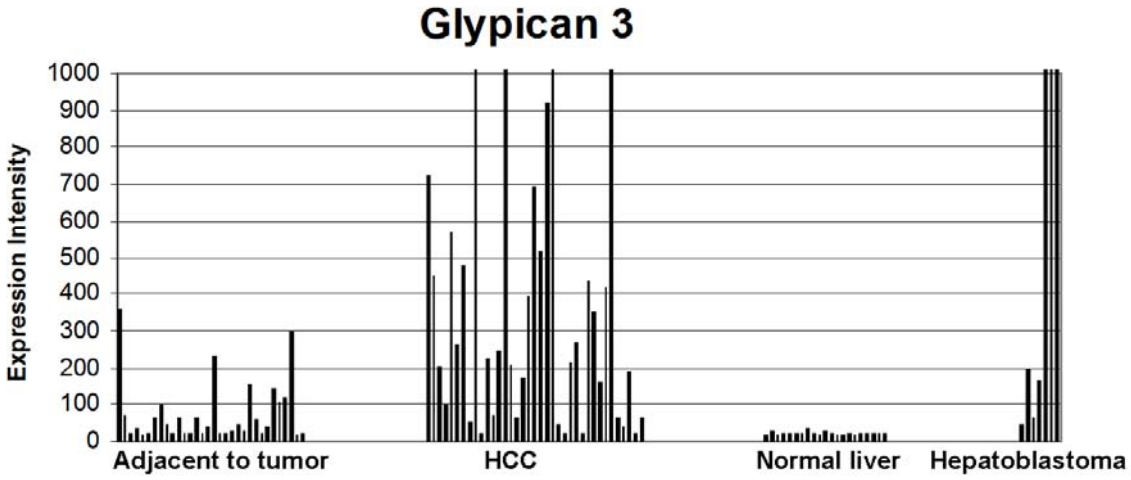

Figure 4. GPC3 Protein Level Varies in Liver Tumor Tissues. AT: adjacent to the tumor; HCC: hepatocellular carcinoma; NL: normal liver; HPBL: hepatoblastoma. Reproduced from reference (18).

It is observed that GPC3 displays a very different expression pattern in tumors (7). Interestingly, the expression of GPC3 is turned on in carcinomas originating from tissues where its expression is low or barely detectable, like HCC and melanoma (22,23). In contrast, its expression is turned down in tumors originating from tissues that normally express it, that is, mammary gland and lung (23,24).

In several malignant tumors, including ovarian carcinoma, cholangiocarcinoma, mesothelioma, and breast cancer, GPC3 is down-regulated as a result of hypermethylation of the GPC3 promoter (25-28). Because the GPC3 protein product is highly expressed in normal ovarian, mammary, and mesothelial cells, GPC3 has been considered a tumor suppressor gene in these organs (27). A multitumor array (MTA) study was used to systematically investigate the epidemiology of GPC3 expression in the liver and in other organs and tissues (Table.1) (29). This tissue specific difference may be due to the fact that GPC3 interacts with different signal pathways and regulates different growth factors in various tissue (30).

Table 1. Multitumor Array (MTA) Results of GPC3 Expression in Tumor Cases. For a total of 347 neoplastic tissue samples demonstrated expression of GPC3 in 15% or more of the studied cases (n ≥ 15). Reproduced from reference (29).

Glypican 3 Expression in Tumors*

Tumor Entity	No. of Cases	No. (%) Staining	
		Negative	Positive
Hepatocellular carcinoma	44	15 (34)	29 (66)
Squamous cell carcinoma of the lung	50	23 (46)	27 (54)
Liposarcoma	29	14 (48)	15 (52)
Testicular nonseminomatous germ cell tumor	62	30 (48)	32 (52)
Cervical intraepithelial neoplasia (grade 3)	29	17 (59)	12 (41)
Malignant melanoma	48	34 (71)	14 (29)
Adenoma of the adrenal gland	15	11 (73)	4 (27)
Schwannoma	46	34 (74)	12 (26)
Malignant fibrous histiocytoma	29	22 (76)	7 (24)
Adenocarcinoma of the stomach (intestinal subtype)	45	36 (80)	9 (20)
Chromophobe renal cell carcinoma	15	12 (80)	3 (20)
Invasive lobular carcinoma of the breast	46	37 (80)	9 (20)
Medullary carcinoma of the breast	30	25 (83)	5 (17)
Squamous cell carcinoma of the larynx	49	41 (84)	8 (16)
Small cell carcinoma of the lung	49	41 (84)	8 (16)
Invasive transitional cell carcinoma of the urinary bladder	43	36 (84)	7 (16)
Mucinous carcinoma of the breast	26	22 (85)	4 (15)
Squamous cell carcinoma of the cervix	41	35 (85)	6 (15)

* Includes all cases with ≥15% positive cases with ≥15 cases tested by multitumor array.

1.1.3 GPC3 Function and Pathways

Despite all the accumulated literature on growth regulation and tumorigenesis by GPC3, its function and mechanisms of action remain elusive. Previous studies have proposed that the unique structure of GPC3, such as the GPI-anchor and HS chains, have played important roles regarding GPC3 function. One possible role of the GPI-anchor is to target the proteins to specific micro-domains within the cell membrane called "rafts" (31), which are highly enriched with sphingolipids, cholesterol, Src family kinases, G proteins, and molecules involved in Ca+ influx (32,33). The targeting of GPC3 to these rafts may therefore facilitate interactions with specific intracellular signaling molecules in the absence of a cytoplasmic domain (2).

On the other hand, GPI-anchored proteins could also be regulated and released into the extracellular environment through the cleavage of GPI linkage by phospholipase C (PLC) (34). It is also suggested that the GPI-anchored proteins are susceptible to unique endocytic pathways that allow them to be remodeled and recycled to the cell surface (35). This recycling for glypicans is accompanied by the remodeling of the GAG chains and the acylation of the GPI anchor to a form resistant to PLC cleavage (35). This process may be associated with receptor-mediated endocytosis (36), which may play a role in the GPC3 pathway.

The modifications in the HS chains of GPC3 are reported to regulate their affinity when interacting with certain ligands, the so called "heparin-binding growth factors (HBGF)" (30), such as fibroblast growth factors (FGFs), Wnts, Hedgehogs (Hhs), bone morphogenetic proteins

(BMPs) (37-40). However, there is evidence that the HS chains are not required for all the activities of GPC3 (41), while the core protein itself could interact with some of those signal molecules and carry out some of the GPC3 functions.

In addition, GPC3 can be cleaved by convertases, generating an ~30 kDa C-terminal subunit containing the heparan sulfate chains and an ~40 kDa N-terminal subunit, the latter being released into the extracellular environment under certain circumstances (42). But the mechanisms of the secreted form of GPC3 may be different from the GPI-anchored cell surface form (6), and the convertase processing of GPC3 may not be required for its activity and signaling pathways (43).

Previous studies suggest that GPC3 is involved in the control of cell proliferation and/or the induction of apoptosis, and may interact with various pathways under normal conditions as well as during carcinogenesis. HSPGs are known to be co-receptors for fibroblast growth factor 2 (FGF2) by promoting FGF-FGFR binding and subsequent activation of the receptor (44,45). It is reported that in HCC, over-expression of GPC3 interacts with FGF2 and inhibits the activity of the receptor (45). Meanwhile, GPC3 can also modulate cell proliferation by inhibiting BMP-7 activity, which is known to control cell proliferation and apoptosis in a dose-dependent manner via Smad1- dependent and -independent pathways (38,46). Previous studies also suggest that GPC3 can stimulate both canonical and non-canonical Wnt signaling pathway in a highly tissue-specific manner (30,47,48). It is reported that GPC3 stimulates HCC growth by facilitating the interaction of Wnt and its receptors, thus activating canonical Wnt pathway (47). This activity of

GPC3 in HCC does not require the presence of HS chains or convertase processing (47,49), but requires attachment of GPC3 to the cell membrane. Therefore, a mutated soluble GPC3 lacking the GPI anchoring domain is able to block Wnt signaling and inhibit the growth of Wnt-dependent tumors (50). On the other hand, the involvement of GPC3 in insulin-like growth factor 2 (IGF2) function and its pathway is still controversial (11,51). These findings suggest that GPC3 does not only regulate cell proliferation under certain conditions but that it also plays an important role in carcinogenesis (38).

1.1.4 Regulation of GPC3

While the function and pathways of action of GPC3 protein are not well characterized, the basis and mechanism for GPC3 gene regulation is also poorly understood. The mechanisms regulating the transcription of GPC3 are of particular importance for understanding the altered expression of GPC3 during development as well as in tumors. Because GPC3 is abundantly expressed in fetal liver and HCC and is silent in the normal adult liver, it is reasonable to postulate that GPC3 is regulated similarly to other genes with the same expression pattern, such as alpha-fetoprotein (*AFP*) and *H19* (52). AFP is a major serum transport protein in the developing mammalian fetus with abundant expression in the fetal liver and is repressed after birth (53,54). During liver regeneration and in HCC, AFP is activated and over-expressed, and is used as a clinical HCC marker (55,56). It is noticeable that GPC3 is activated more often than AFP in small dysplastic liver nodules, and thus more valuable for early diagnosis of HCC (57,58). *H19* encodes an un-translated mRNA of unknown function, with a similar expression pattern to *AFP* (59).

From the insight into the regulation of *AFP* and *H19*, previous studies have suggested that zinc finger and homeoboxes 2 (Zhx2) repress GPC3 in the adult liver, and might also be involved in GPC3 activation in HCC (52). Alpha-fetoprotein regulator 2 (Afr2) could also reactivate GPC3 expression in regenerating liver after carbon tetrachloride (CCl4) intoxication (52). It is also reported that sulfatase 2 (SULF2) has an oncogenic effect in HCC mediated in part through up-regulation of FGF signaling and GPC3 expression (60).

As the GPC3 gene is located on the X chromosome and DNA methylation is implicated in chromosome X inactivation (61), methylation of the GPC3 promoter was examined with little evidence found correlating methylation and expression of GPC3 (62). But an *in vitro* study showed that the transcriptional activation of the GPC3 gene requires an absence of methylation of the gene promoter, Although the absence of methylation alone does not necessarily lead to transcriptional activity (63). Overall, the pattern and mechanism for GPC3 expression regulation still remains to be discovered.

1.2 LIVER REGENERATION

The liver is the second largest organ (the largest is the skin) and the largest gland in the human body. Medical terms of “hepato-” or “hepatic” come from the Greek “hepar” (ήπαρ) for liver.

The liver is a complex, indispensable, multipurpose organ, the major role of which is dealing with the nutrient products of food digestion and detoxifying harmful substances absorbed via the intestine (64). The liver is also the only organ involved in production of bile, which is important in the breakdown and absorption of fats and lipophilic substances such as many vitamins. Another role of the liver is producing essential proteins and clotting factors for the blood, and regulation of the metabolism of cholesterol and glucose (65,66).

1.2.1 Liver Architecture

At the microscopic level, the liver consists of subunits of a roughly hexagonal arrangement, called hepatic lobules, mainly made up of plates of hepatocytes radiating outward from a central vein (67) (Fig.5). Between the radiating rows of hepatocytes are small blood vessels called sinusoids. These receive oxygen-rich blood from the hepatic artery and nutrients from the intestines via the portal vein. The oxygen and nutrients diffuse through the capillary walls into hepatocytes (64). The endothelial cells of the hepatic sinusoids are “fenestrated”; they have pores that allow direct access of plasma to the underlying hepatocytes. At the corner of each lobule is the portal area (portal triad), composed of branches of the hepatic portal vein, hepatic artery, bile duct, and nerves. Bile drains from the hepatocyte bile canaliculi into the many small bile ducts that unite to form the main bile duct of the liver (the hepatic duct). This joins the cystic duct, which leads from the gallbladder, to form the common bile duct, which drains into the duodenum. The central lobular veins are blood vessels which receive blood from the hepatic portal vein and hepatic artery via the sinusoids and then drain the blood into the hepatic vein (64).

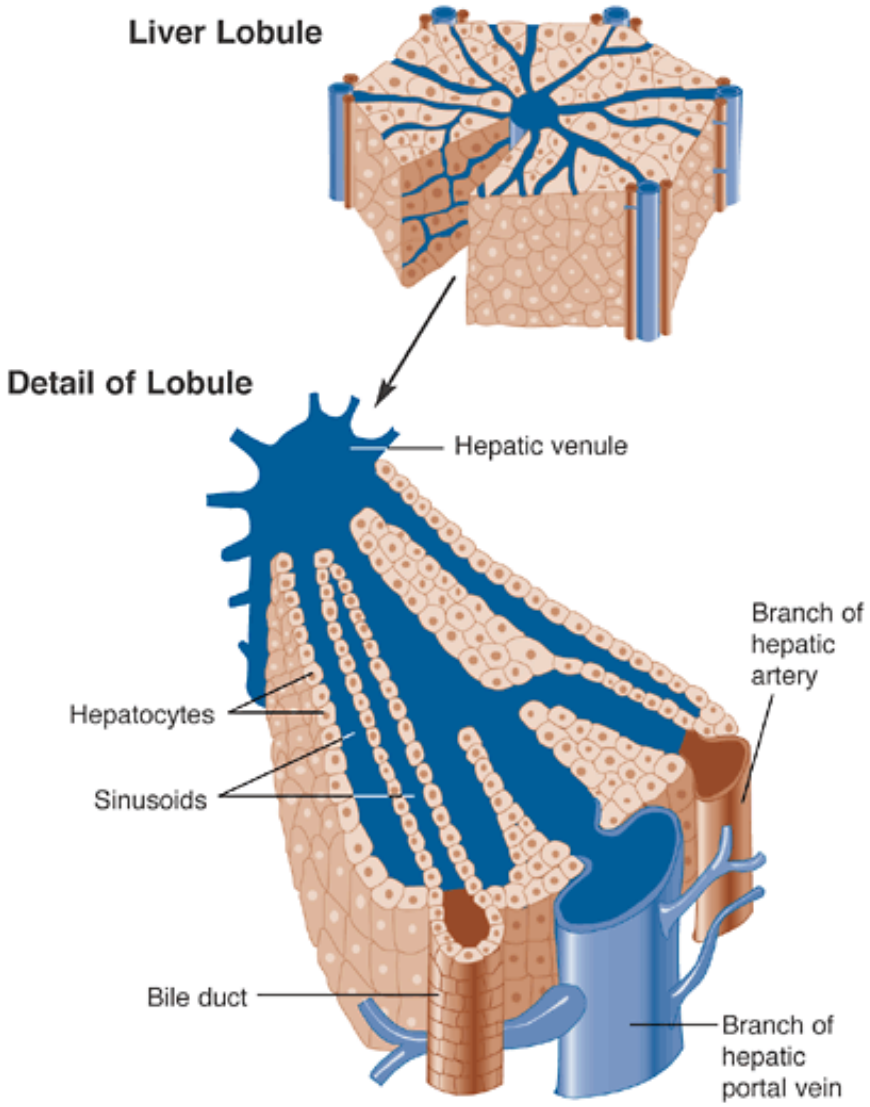

Figure 5. The Structure of the Liver's Functional Units, or Lobules. Blood enters the lobules through branches of the portal vein and hepatic artery, then flows through small channels called sinusoids that are lined with primary liver cells (i.e., hepatocytes). The hepatocytes remove toxic substances, including alcohol, from the blood, which then exits the lobule through the central vein (i.e., the hepatic venule). Reproduced from reference (67).

1.2.2 Liver Cell Types

The liver consists of both parenchymal cells (hepatocytes) and non-parenchymal cells (Stellate cells or Ito cells, Kupffer cells, biliary epithelial cells or cholangiocytes, and sinusoidal endothelial cells) (68,69), as described below:

Hepatocytes: account for 80% of the liver cell population and carry out the major functions of the liver. Hepatocytes are large, hexagonally-shaped, polyploid cells arranged in thin layers that radiate from the central canal (central vein) to the periphery of the lobule (portal triad). Hepatocytes are involved in protein synthesis, protein storage, transformation of carbohydrates, synthesis of cholesterol, bile salts and phospholipids, producing clotting factors and serum albumin, detoxification, modification, and excretion of exogenous and endogenous substances, and initialization of the formation and secretion of bile.

Stellate cells or Ito cells: represent 5-8% of the total population of liver cells. They are pericytes found in the liver perisinusoidal space (a small area between the sinusoids and hepatocytes), which store fat and vitamin A and produce certain growth factors such as Hepatocyte Growth Factor (HGF) and Transforming Growth Factor β1 (TGFβ1). The stellate cells also produce connective tissue proteins and are the major cell type involved in liver fibrosis.

Kupffer cells: specialized macrophages located in the lining of the walls of the sinusoids, which break down red blood cells and destroy microbes and foreign substances by phagocytosis.

Kupffer cell activation is responsible for early ethanol-induced liver injury, common in chronic alcoholics. The other immune cells in the liver belong to the adaptive immune system (T and B lymphocytes) and the innate immune system (natural killer cells, and natural killer T cells).

Biliary epithelial cells or cholangiocytes: cuboidal epithelium in the small interlobular bile ducts, but become columnar and mucus secreting in larger bile ducts approaching the porta hepatis and the extrahepatic ducts.

Sinusoidal endothelial cells: the thin layer of cells that line the interior surface of blood vessels, comprising approximately 50 % of the non-parenchymal cells. They separate hepatocytes from the passing blood and play an important role in hepatic microcirculation. These cells lack a basement membrane, form a fenestrated monolayer, express a variety of scavenger receptors, and control the exchange of material between the blood and the liver parenchyma.

1.2.3 Liver Regeneration and Partial Hepatectomy (PHx) Model

Liver has great potential to regenerate, which is a fundamental parameter of liver response to injury. Liver regeneration may be defined as, "…An orchestrated response induced by specific external stimuli and involving sequential changes in gene expression, growth factor production and morphologic structure…" (68,69). Unlike other regenerating tissues, such as bone marrow

and skin, liver regeneration under normal circumstances does not depend on a small group of progenitor or stem cells, but the proliferation of hepatocytes (68,69).

In modern times, the best experimental model for the study of liver regeneration is the 2/3 partial hepatectomy models (70), in which specific liver lobes that account for about 2/3 of the total mass are removed intact and the residual lobes enlarge to make up for the loss of mass (Fig.6) (71). Partial hepatectomy is often used to study liver regeneration because, compared with other methods that use hepatic toxins (such as CCl_4), it is not associated with tissue injury and inflammation, and the initiation of the regenerative stimulus is precisely defined (removal of liver lobes) (68,69). The residual lobes enlarge to make up for the mass of the removed lobes, though the resected lobes never grow back.

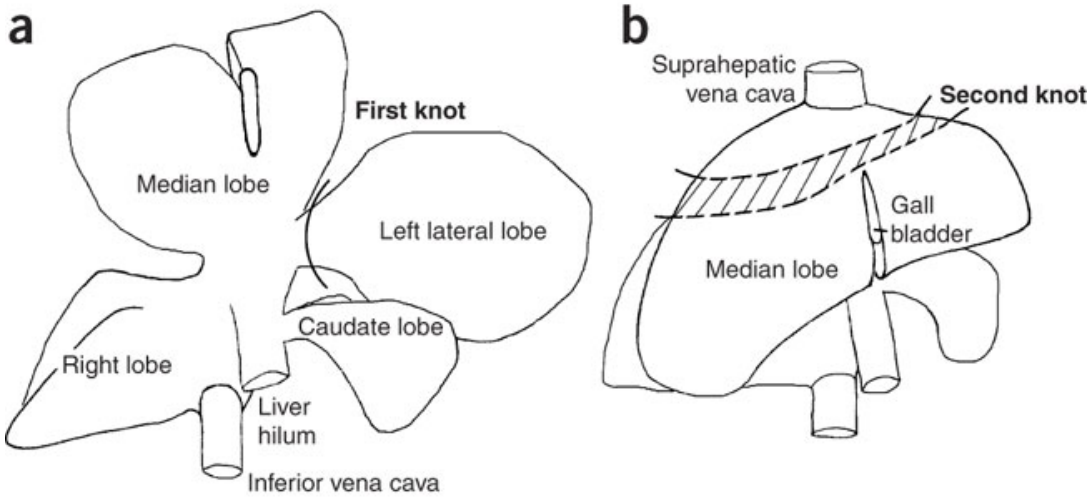

Figure 6. Schematic Drawings of Mouse Liver Anatomy and PHx Procedure. (a) The thread for the first knot should be positioned between the caudate and the left lateral lobes at the base of the latter. (b) The second knot should be tied within the dashed area, above the gall bladder but not too close to the suprahepatic vena

cava. The tip of the right lobe can be used as a reference point for placing the knot. Reproduced from reference (71).

Following liver PHx, hepatocytes enter into the cell cycle from their habitual quiescent phase and proliferate to restore normal hepatic mass and hepatic functional capacity (68). The whole process lasts about 5 to 7 days in rats and mice, during which hepatocytes are the first cells to enter into DNA synthesis from their habitual quiescent phase at about 24 hours post-PHx in rats. Hepatocyte proliferation starts in the areas of the lobules surrounding the portal triads (periportal) and proceeds to the pericentral areas (69,72), followed by the biliary ductular cells, then the Kupffer cells and stellate cells, and finally the endothelial cells (Fig.7) (68).

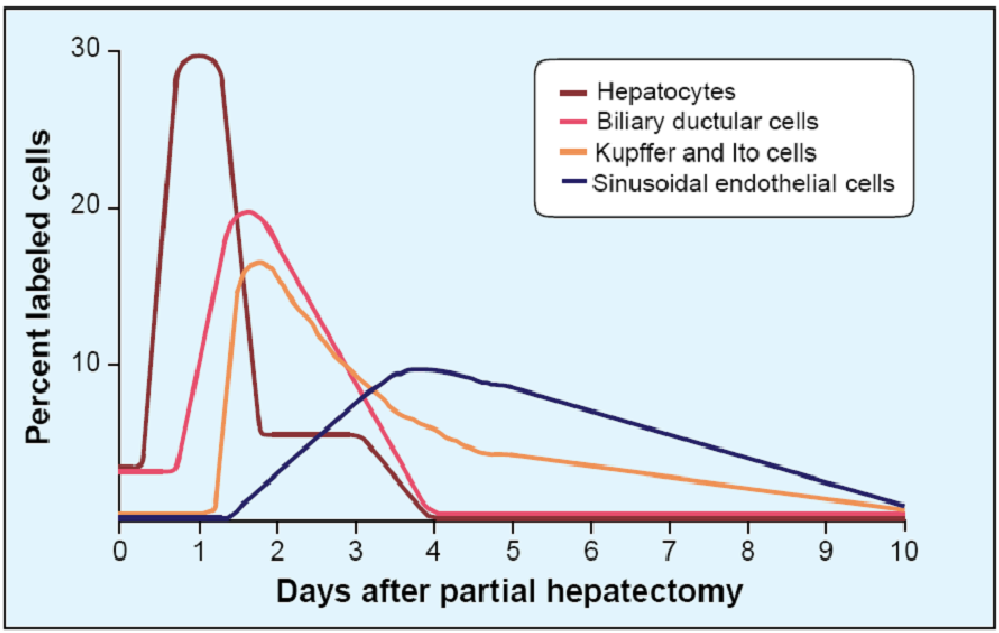

Figure 7. Time Kinetics of DNA Synthesis in Different Liver Cell Types during Liver Regeneration after Partial Hepatectomy. The four major types of liver cells undergo DNA synthesis at different times. Hepatocyte DNA synthesis peaks at 24 hours, whereas the other cell types proliferate later. Reproduced from reference (68).

1.2.4 Mitogenic Signals and Pathways

The liver regenerative process is associated with signaling cascades involving growth factors, cytokines, matrix remodeling, and several feedback points between stimulation and inhibition of growth related signals (68). During this process, several growth factors and cytokines plays important roles, including hepatocyte growth factor (HGF), epidermal growth factor (EGF), transforming growth factor-α (TGF-α), tumor necrosis factor-α (TNF-α), interleukin-6 (IL-6), insulin, and norepinephrine (Fig.8) (68,69,73).

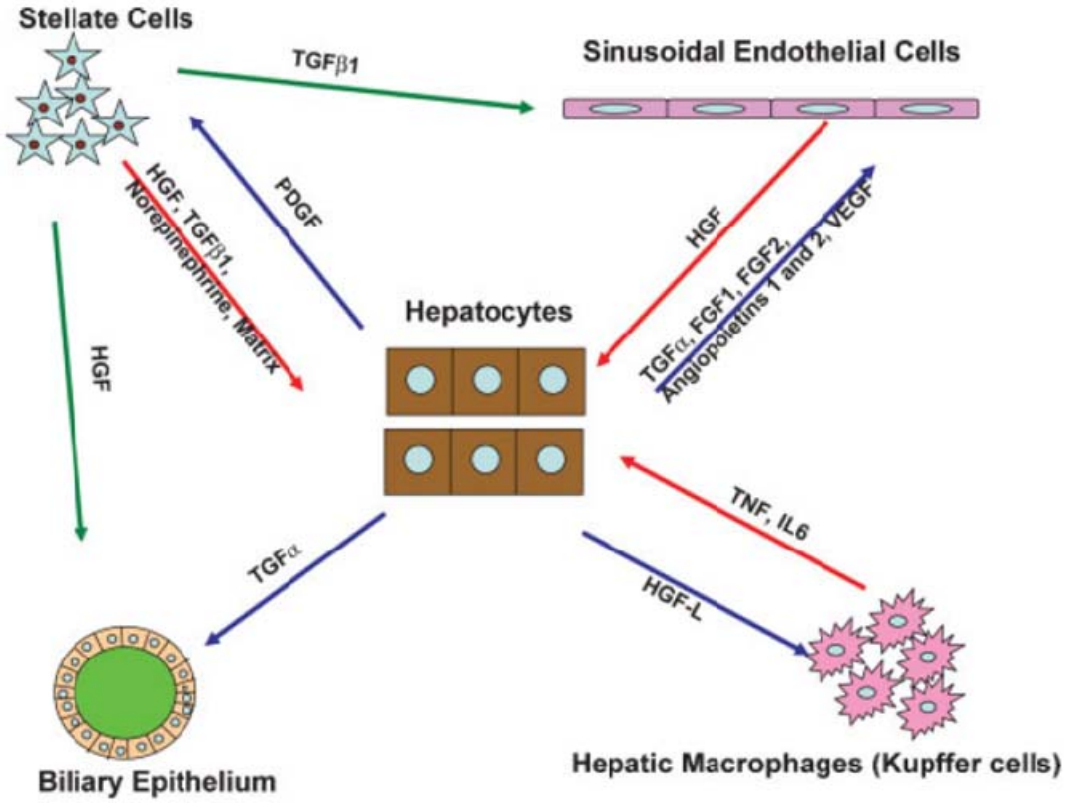

Figure 8. Signaling Interactions between Different Hepatic Cell Types during Liver Regeneration. Reproduced from reference (68).

PHx induces rapid induction of more than 100 genes not expressed in normal liver (74). The exact role of each gene may not be fully characterized, but the early changes in gene expression should be viewed as serving both the entry of hepatocytes into the cell cycle and the orchestration of specific adjustments that hepatocytes have to make, so that they can maintain all essential hepatic functions while going through cell proliferation (68,69).

The early events are associated with extracellular matrix (ECM) remodeling and activation of locally bound growth factors as well as receptors (Fig.9) (75). While there is not much proteinaceous matrix in the liver visible under the microscope, there is a great abundance of heavily glycosylated proteins in the pericellular space surrounding hepatocytes (68). One of the earliest observations after PHx is the increase in the activity of urokinase-type plasminogen activator (uPA), accompanied by activation of scHGF (single-chain HGF) to HGF (76). Urokinase is known to activate matrix remodeling during liver regeneration, and many proteins and growth factors in the extracellular matrix are subject to turnover (77). During this process, the inactive form of sc-HGF is hypothesized to be locally released from the hepatic biomatrix prior to its activation by uPA to its functional heterodimeric form (76,78). Regardless of when activation occurs, release and activation of HGF further leads to activation of cMet, the HGF receptor, between 5 and 60 minutes after PHx (79).

It has also been observed that TGFβ1, a known hepatocyte mitoinhibitor, is also released locally and in the peripheral circulation shortly after PHx (79). This suggests that matrix remodeling alters the balance of mitogens and mitoinhibitors formed in the hepatic quiescence state and

triggers the regeneration process (68). The EGFR is also activated after PHx, with the same kinetics as Met (79). An increase in the concentration of other signaling molecules in plasma is observed after PHx, such as TNF, IL6, bile acids, norepinephrine and serotonin (68), which play important roles during liver regeneration.

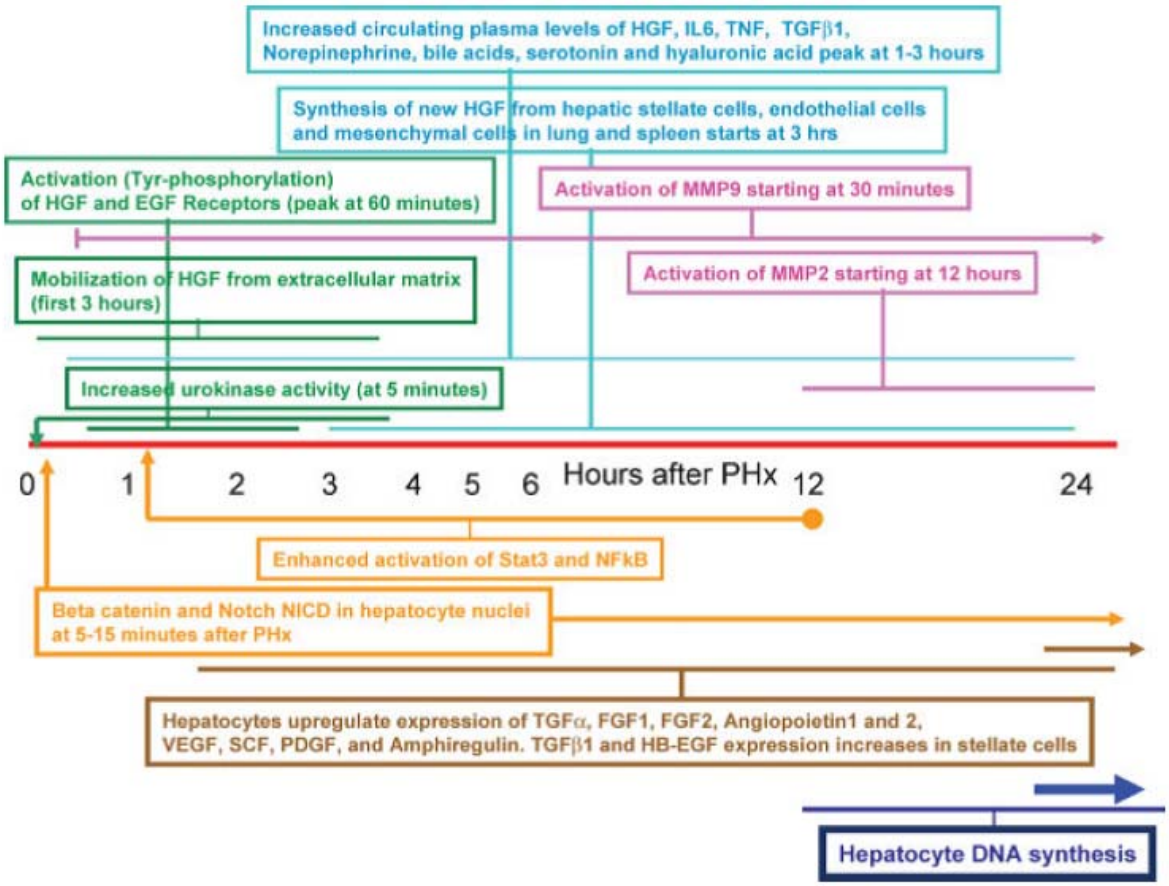

Figure 9. Chronology of Key Events Occurring at the Early Stages of Liver Regeneration after Partial Hepatectomy. Events within similarly colored boxes belong in the same category (e.g., green: growth factor related events; blue: plasma related changes, etc.). The associated horizontal lines for each box delineate the beginning and the duration of each signal. Reproduced from reference (68).

Besides the early changes and remodeling in the extracellular matrix, there are many events occurring inside the cells (Fig.9) (68). There is evidence of activation and translocation of the transcription factor signal transducer and activator of transcription-3 (STAT3) (80) and nuclear factor kappa B (NF-κB) (p50-p65 complex) within 1 hour after PHx, which activates many of the immediate early genes (69). Beta catenin (81) and the Notch-1 intracellular domain (NICD) (82) also appear in hepatocyte nuclei within 15–30 min after PHx. As a result of new synthesis of both c-Fos and c-Jun, the Jun-Fos complex known as activator protein 1 (AP1) activity also increases rapidly after PHx (83). LRF-1, another leucine zipper protein, is also induced rapidly after PHx and participates in complex formation with c-Jun (83). Activation of STAT3, NF-κB, and AP1 is likely to be a major part of the intracellular signaling cascade leading to DNA synthesis. At 6 h after PHx there is clear evidence for activation of cyclin D1 (84). There is a decrease in CCAAT-enhancer-binding protein α (C/EBPα) amounts and an increase in C/EBPβ, a process thought to be underlying some of the shifts in metabolism that occur during liver regeneration (85). Additional "hepatic-associated" transcription factors such as hepatic nuclear factor 1 (HNF1), HNF4, HNF3, and others remain essentially unchanged (69).

1.2.5 Termination of Liver Regeneration

After all cellular elements of the liver proliferate, the liver histology is gradually rearranged and restored toward the end of the liver regeneration process (69). At days 3 to 4 after PHx the liver is characterized by clumps of small hepatocytes surrounded by capillaries. The stellate cells send processes that penetrate the hepatocyte clumps and start producing several types of laminin (86).

Eventually, the small hepatocyte clumps become rearranged into the typical hepatocyte plates seen in the mature liver (69,86). The capillaries of the small hepatocyte clumps (surrounded by typical capillary basement membrane) change into true hepatic sinusoids (surrounded by very scant matrix and lined by fenestrated endothelial cells and Kupffer cells) (68,69). The hepatic matrix composition also changes from high laminin content to very scant matrix containing primarily fibronectin, collagen types IV and I, and several other proteins and glycosaminoglycans in smaller amounts (69). Normal liver weight, not exceeding the original size, is reestablished within 5-7 days in rats and mice (8-15 days in humans). At the end of regeneration, the size of the liver lobules is remarkably larger and the thickness of the hepatocyte plates is almost twice the size of the normal one cell thickness (68,69). Previous studies suggest that a small wave of apoptosis in hepatocytes occurs at the end of regeneration (87), and liver lobules are slowly reorganized so that eventually liver histology becomes indistinguishable from the original (88).

Most previous studies have focused on the initiation of liver regeneration while much less has been studied about the termination of liver regeneration, although it is equally if not more important. It is reasonable to speculate that the reassembly of the extracellular matrix and the sinusoidal capillary network provides matrix-driven signaling that terminates the regenerative process (Fig.10). This may be direct signaling through integrins (89) or signaling induced by TGFβ1 (bound to the newly synthesized decorin and again exerting a ‘‘tonic’’ mito-inhibitory effect) (68,69). Synthesis of new decorin, perlecan, and syndecan and collagen types I and III dramatically increases during regeneration (90,91). Newly synthesized matrix would also be capable of binding HGF, which has high affinity to glycosaminoglycans and heparin, thus

preventing it from being activated by urokinase (92). This set of events would bring hepatocytes back into a state of quiescence, surrounded by HGF (bound to glycosaminoglycans) and TGFβ1 (bound to decorin). After PHx, early mitogenic stimuli such as HGF and EGF drive both hepatocyte proliferation and enhanced expression of TGFβ1. While proliferating hepatocytes become resistant to TGFβ1, TGFβ1 stimulates production of extracellular matrix in stellate cells, formation of hepatic sinusoids, and leads to inhibition of urokinase and HGF activity (93). New extracellular matrix synthesis by stellate cells restores binding of both HGF and TGFβ1 and reestablishes quiescence of hepatocytes towards the end of liver regeneration (68,69).

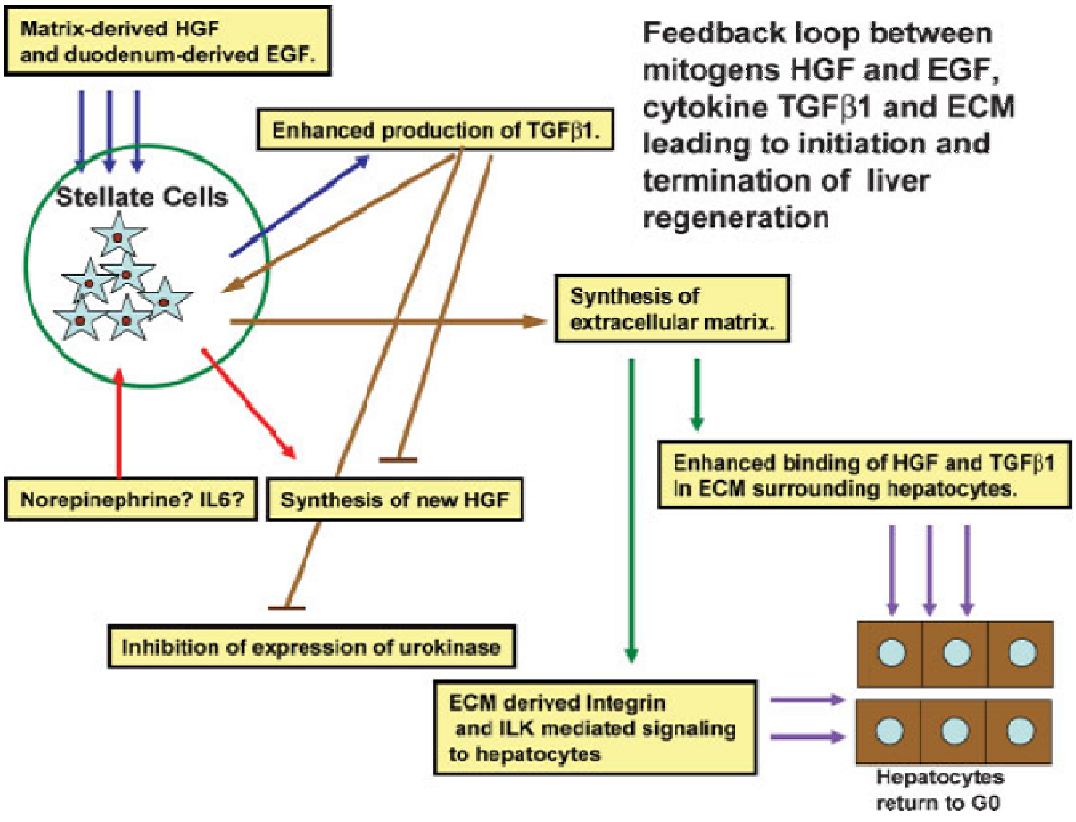

Figure 10. Schematic of a Feedback Loop between Growth Factors, TGFβ1, and Extracellular Matrix, Controlling Early and Late Stages of Regeneration. Mitogens (HGF and EGF) upregulate expression of TGFβ1 by stellate cells. The latter stimulates synthesis of new extracellular matrix, while eventually blocking

synthesis of new HGF and expression of urokinase. The newly synthesized extracellular matrix supports binding of single chain HGF and TGFβ1 around hepatocytes and restoration of quiescence (G0 phase). Arrows of the same color denote similar origin of the input and output of the same signaling process. Reproduced from reference (68).

Hence, overall, TGFβ1 is not a direct terminator of regeneration but it orchestrates multiple events after PHx (68), with the underlying mechanism and overall impact of TGFβ1 still not clear. Other potential metabolites, growth factors, cytokines and matrix proteins are also proposed to play a role in the termination of liver regeneration, but no specific terminator is known and to date, less is understood about the signaling pathways toward the end of liver regeneration.

2.0 INVESTIGATION OF THE ROLE OF GLYPICAN 3 IN RAT LIVER REGENERATION AND HEPATOCYTE PROLIFERATION

Since loss of function in GPC3 in SGBS and GPC3-/- mice leads to overgrowth of many organs, including liver, it is reasonable to speculate that GPC3 normally functions as a growth inhibitor in the liver. Given the over-expression of GPC3 in HCC, we wanted to study the role and mechanisms of GPC3 signaling in normal liver regeneration and hepatocyte growth regulation. To this end, we used the rat model of liver regeneration after partial hepatectomy (PHx) in which hepatocyte growth dynamics are well characterized (68). We also used hepatocyte primary cultures, in which we and others have characterized the hepatocyte growth cycle under the influence of hepatocyte growth factor (HGF) and epidermal growth factor (EGF) (94). Our study demonstrated that GPC3 mRNAs and proteins increase in a time frame that coincides with the termination of proliferative activities of either hepatocytes (day 2 after PHx and day 8-12 in culture) or NPCs (day 5-6 after PHx). *In vitro* studies showed that hepatocyte growth was promoted when GPC3 expression was blocked using antisense morpholino oligonucleotides. The yeast two-hybrid assay revealed that GPC3 interacts with CD81, a cell membrane tetraspanin,

which was further confirmed by co-immunofluorescence and co-immunoprecipitation studies. CD81 mRNA and protein increase in grossly the same time frame after PHx. The co-localization of GPC3 and CD81 at days 2 and 6 after PHx indicated the potential for an important regulatory interaction between the two proteins.

2.1 MATERIALS AND METHODS

2.1.1 Rat Partial Hepatectomy Model

Male Fisher344 rats (150–200 g) were purchased from Charles River Laboratories (Frederick, MD). Animals were allowed access to food and water *ad libitum*. Isoflurane inhalation (Baxter, IL) was used to anesthetize animals. In the PHx model, the median and left lateral lobes (accounting for 2/3 of the total liver mass) were resected (79). The remaining liver lobes were obtained from defined time points after PHx at 1, 2, 3, 4, 5, 6, and 7 days. Liver samples were promptly frozen in liquid nitrogen and stored at -80°C. Fresh rat liver tissue was also placed in Tissue-Tek OCT embedding compound, frozen on dry ice, and stored at -80°C. All animals were housed in the animal facility at the University of Pittsburgh, and all procedures performed on these rats were approved under the IACUC protocol and conducted according to National Institutes of Health guidelines.

2.1.2 Cell Culture and Proliferation Assay

Hepatocytes were isolated from normal Fisher344 rats by an adaptation of Seglen's calcium 2-step collagenase perfusion technique (79) as previously described from our laboratory (95). Isolated rat hepatocytes were added to collagen-coated six well plates (BD Biosciences, CA, USA). Each well contained 200,000 freshly isolated hepatocytes in 1 mL hepatocyte growth medium (HGM) supplemented with HGF (40 ng/ml) and EGF (20 ng/ml). ^{3}H-thymidine was added to the medium for 48 hours at a concentration of 2.5 μCi/ml. The medium was removed at defined time points, and hepatocytes were fixed with ice cold 5% TCA. Then TCA was removed and the plates were washed in running tap water, and air dried completely. 500 ul 0.33N NaOH was added to each well for 30 minutes to solubilize the cells. The solution was transferred into a new tube and 166ul 20% TCA/1.2N HCl was added for precipitation. The tubes were centrifuged at maximum speed for 10 minutes, and the pellets were re-dissolved in 500 ul 0.33N NaOH. A 200 ul aliquot was used to measure the CPM/DPM in Beckman LS6000IC scintillation counter (Beckman Coulter, CA, USA), and 100 ul was used to determine the OD value of total DNA.

2.1.3 RNA Extraction and Semi-Quantitative RT-PCR

RNA was extracted from frozen liver tissues with Trizol (Invitrogen, CA, USA) according to the manufacturer's instructions. 5 ug of RNA was reverse-transcribed to complementary DNA (cDNA) with SuperScript III reverse transcriptase (Invitrogen, CA, USA) according to the standard protocol. Standard PCR was performed with Taq polymerase (Qiagen, CA, USA). The

primers used to perform PCR are: GPC3-Forward: GGTGACGGCATGATGAAAGTGAAG; GPC3-Reverse: TGGTGATCTCGTTGTCCTTCTGAT; CD81-Forward: CGCGGTACCATGG GGGTGGAGGGCTGCAC; CD81-Reverse: CCGGAATTCTCAGTACACGGAGCTGTTCCG G. The PCR products were resolved on 2 % agarose gels and visualized with ethidium bromide staining, and digital images were quantitated using NIH ImageJ software.

2.1.4 Protein Extraction and Western Blotting

Frozen liver tissue and hepatocytes were homogenized in RIPA buffer (50mM Tris-HCl, pH 7.4, 150mM NaCl, 0.1% SDS) supplemented with proteinase inhibitors. For HS chain elimination, 100 ug protein extract from freshly isolated rat hepatocytes and total rat liver was treated with 5 microunits heparitinase enzyme (Seikagaku, Tokyo, Japan) and 1 mM $CaCl_2$ for 3 hours (73). Protein samples (20 ug) were resolved on 4% to 12% NuPage Bis-Tris gels with 1X MOPS running buffer (Invitrogen, CA, USA), then transferred to Immobilon-P membranes (Millipore, MA, USA) in NuPAGE transfer buffer containing 10 % methanol. Membranes were stained with 0.2 % Ponceau Red to verify loading and transfer efficiency. Membranes were then probed with primary and secondary antibodies in TBST buffer (Tris-buffered saline Tween 20) containing 5 % nonfat milk, then processed with SuperSignal West Pico chemiluminescence substrate (Pierce, IL, USA) and exposed to a X-ray film (Lab Product Sales, NY, USA).

2.1.5 Knocking Down GPC3 using Morpholino Oligos

Morpholino antisense oligos targeted to translational start sites of rat GPC3 were designed and synthesized by Gene Tools, LLC (Philomath, OR, USA). The morpholino oligo sequence complementary to the translational-blocking target GPC3 is: 5'-3' CACGGTCCCGGCCATCCT GCTTCTT. The Morpholino was complexed with the Endo-Porter delivery reagent, which is used to deliver "bare" oligos by an endocytosis-mediated process (96). Rat hepatocytes were isolated and plated into collagen coated six well plates. In brief, 1 ml of HGM with HGF and EGF was combined with 20 µl of 1 mM Morpholino oligos and 5 µl of 1mM Endo-Porter dissolved in DMSO, and applied to cell cultures in six-well plates for 48 h. Endo-Porter solution alone was added as a negative control. After the allotted time period, the medium was removed and replaced with fresh HGM with HGF and EGF. For six-day experiments, Morpholino oligos and Endo-Porter reagent were added at days 2 and day 4. ^{3}H-thymidine assays were performed as described in 2.1.2. All transfection experiments were carried out in triplicate. GPC3 protein levels for each time points were determined by western blotting.

2.1.6 Yeast Two-Hybrid Assay

The matchmaker GAL4 yeast two-hybrid system (Clontech, CA, USA) was used for identification of GPC3-binding proteins, according to standard protocol (97). As bait for screening, the vector pGBKT7 expressing a fusion protein composed of full-length rat GPC3 cDNA linked to the DNA-binding domain was constructed. A rat liver cDNA library was cloned

into the pACT2 vector containing a GAL4 activation domain. Both of the vectors were used to transform the AH109 yeast strain. Positive clones were selected on SD/-Ade/-His/-Leu/-Trp high stringency YPDA plates with X-gal. Plasmids from positive clones were subsequently isolated from the yeast, transferred to *E. coli* Top10 competent cells (Invitrogen, CA, USA), and sequenced. The GenBank/NCBI databases were screened for similar sequences using a BLAST Search.

2.1.7 Co-Immunoprecipitation

Normal rat liver tissue was lysed in RIPA buffer as described above. For immunoprecipitation studies, 500 ug of protein lysates were diluted to a final volume of 500 ul and pre-cleared by incubating with 1 ug hamster IgG (Santa Cruz, CA, USA) and 20 ul agrose A/G plus beads (Santa Cruz, CA, USA) for 1 hour at room temperature. Protein complexes were immune-precipitated from cleared lysates with 1 ug of anti-CD81 monoclonal antibody (GeneTex, TX, USA) overnight at 4 °C, followed by a 5-hour incubation at 4 °C with agarose A/G plus beads. Immune-complexes were then collected and washed three times with RIPA buffer, prior to resuspension in 4X SDS-PAGE sample buffer and 1X Reducing Reagent (Invitrogen, CA, USA). Proteins from either immunoprecipitated samples or 20 ug of crude liver protein were separated by SDS-PAGE, and subjected to western blotting using antibody against GPC3 (Aviva, CA, USA). All protein bands were detected using western blotting as described above.

2.1.8 Co-Immunofluoresence

Frozen rat liver sections (5 μM) were fixed in ice cold 100 % acetone for 5 minutes, blocked with 5 % normal goat serum in PBS for 2 hours, and co-stained successively using primary antibodies against GPC3 (Aviva, CA, USA) and CD81 (GeneTex, TX, USA). GPC3 rabbit antibody (4 ug/ml) was incubated over night at 4°C, washed, and followed by incubation using CD81 hamster antibody (1.25 ug/ml) for 2 hours at room temperature. The two fluorescent conjugated secondary antibodies were goat-anti-rabbit (Alexa 488) at a dilution of 1:500, and goat-anti-hamster (Cy3) antibody at a dilution of 1:1000. Sections were counterstained with the nuclear DNA probe DRAQ5 (Biostatus Limited, UK) at a dilution of 1:1000 dilution. Images were visualized using Nikon Eclipse confocol fluorescent microscope.

2.2 RESULTS

2.2.1 GPC3 Protein and RNA Levels Increase during Liver Regeneration

During rat liver regeneration following PHx, different cell types proliferate at different times and the entire process usually finishes within 7 to 10 days. To study the role of GPC3 in liver regeneration, we first investigated the mRNA and protein levels of GPC3 during this process. Semi-quantitative RT-PCR results showed that GPC3 expression increases from day 2 after rat PHx with a peak at day 5 (Fig.11A). Western blot analysis revealed that GPC3 protein started increasing from day 2 after PHx, peaked at day 5, and decreased at day 6, corresponding with the RT-PCR results (Fig.11B).

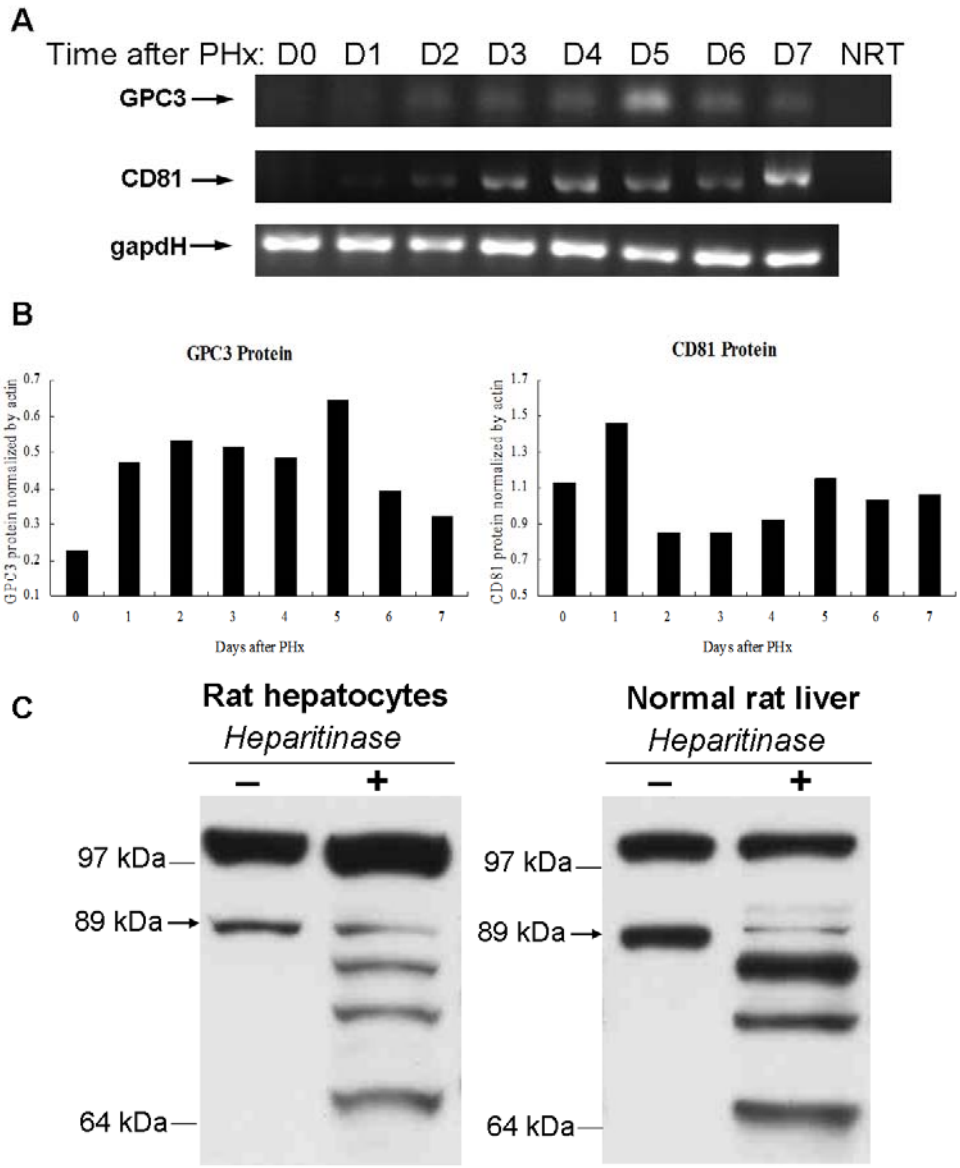

Figure 11. RNA and Protein Levels of GPC3 and CD81 increase during Liver Regeneration. (A) Semi-quantitative RT-PCR results show that GPC3 and CD81 expression are elevated in PHx after day 2. GAPDH: loading control. NRT: non-RT negative control. (B) GPC3 and CD81 protein levels, normalized by actin, increase from day 2 after PHx with a peak expression at day 5. (C) Western blotting results of GPC3 protein extract from freshly isolated normal rat hepatocytes and normal rat liver tissue treated with heparitinase to eliminate HS chains. The arrow indicates the 89 kDa glycosylated form of GPC3.

It is reported that the core protein of GPC3 is 67.5 kDa in size. However, in our western blotting an 89 kDa band was detected by the rabbit anti mouse GPC3 polyclonal antibody. In view of the fact that GPC3 is highly glycosylated, to verify the 89 kDa band was GPC3, we treated the protein samples from freshly isolated rat hepatocytes as well as normal rat liver extract with heparitinase to eliminate the HS chains. After a 3-hour treatment with heparitinase, the intensity of the 89 kDa protein band diminished and a series of bands appeared including the 67 kDa GPC3 core protein band (Fig.11C). The multiple protein bands which appeared after heparitinase treatment may be due to incomplete digestion. These results are consistent with the reported high glycosylation levels of GPC3 protein.

2.2.2 GPC3 Increases at the End of Hepatocyte Proliferation

We further investigated GPC3 in hepatocyte cultures. Rat hepatocytes were isolated from normal rat liver and incubated with HGF and EGF, to stimulate cell proliferation in culture. DNA synthesis was detected using a ^{3}H-thymidine incorporation assay, and hepatocyte proliferation (^{3}H-thymidine count per mg DNA) was determined (Fig.12). The ^{3}H-thymidine incorporation assay shows a peak of hepatocyte proliferation at day 7, and then DNA synthesis slows down. Western blotting showed that GPC3 levels, normalized by β-actin control, start increasing around day 7 (Fig.12), which correlated with the beginning of the decrease in hepatocyte DNA synthesis.

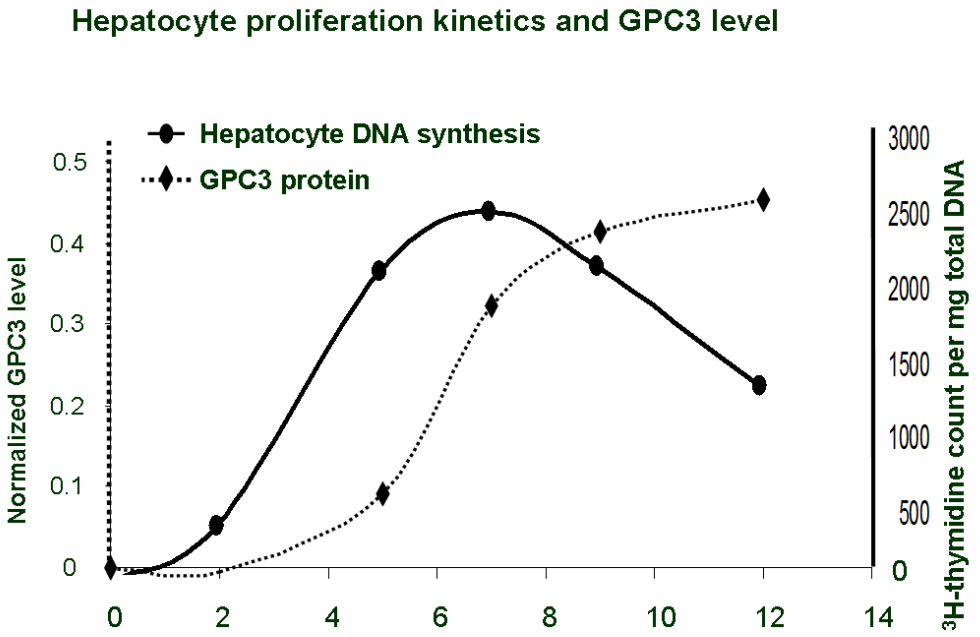

Figure 12. GPC3 Levels Increase when DNA Synthesis Stops in Rat Hepatocyte Culture. 3H-thymidine incorporation per mg total DNA (solid line) and GPC3 level (dotted line) for different time points in hepatocyte culture are shown.

2.2.3 Knocking Down of GPC3 by Morpholino Oligos Promotes Hepatocyte Growth at the End of Proliferation

To determine the role of GPC3 in liver regeneration, Morpholino oligos were used to knock down GPC3 protein expression in hepatocyte cultures. Morpholino oligos against GPC3 were commercially synthesized and added together with Endo-Porter reagent at day 0 and day 4 in hepatocyte cultures. To study the growth and proliferation of hepatocytes, ^{3}H-thymidine counts and total DNA were collected for each time point. Growth curves were created according to ^{3}H-

thymidine counts (Fig.13A) or total amount of DNA (Fig.13B) for hepatocytes with GPC3 Morpholino oligos or only with Endo-Porter control. In cultures with Morpholinos, both ^{3}H-thymidine counts and total DNA increase at day 6, when cell proliferation in control cultures slows down. Western blotting results showed that GPC3 protein is reduced at day 4 and 6 in hepatocytes cultured with GPC3 Morpholino oligos, but not with Endo-Porter control (Fig.13C).

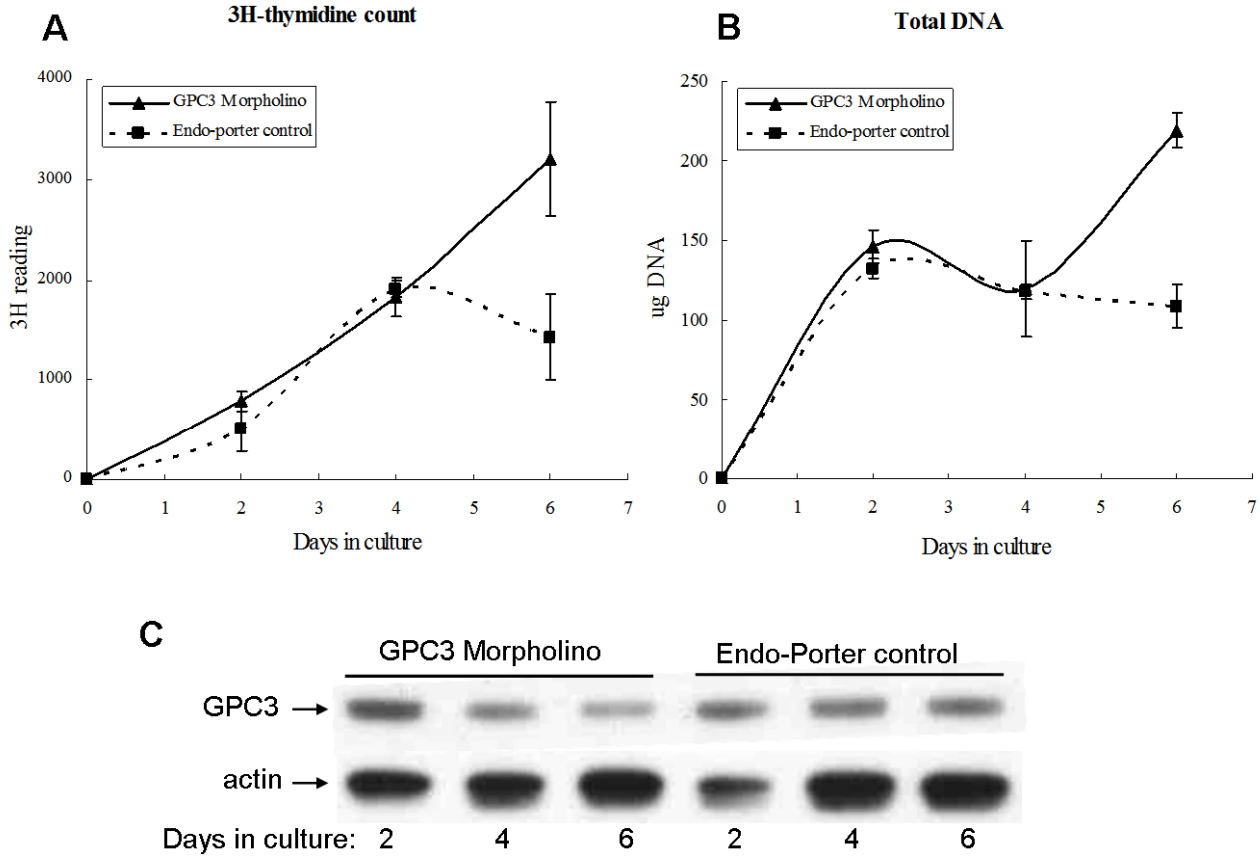

Figure 13. Effect of GPC3 Morpholino and Endo-Porter Control on 3H-thymidine Up-take (A) and Total DNA (B) in Rat Hepatocyte Cultures. All experiments were carried out in triplicate, and standard error is indicated by the error bars. GPC3 Morpholino promoted hepatocyte growth at day 6. (C) GPC3 protein is knocked down in cell cultures treated with GPC3 Morpholino oligos but not with Endo-Porter control, as shown by western blotting.

2.2.4 GPC3 and CD81

To screen for proteins that might interact with GPC3, a yeast two-hybrid assay was performed. Several interesting genes were found, such as a tyrosine kinase substrate (Hrs), prostaglandin D2 synthase (Ptgds), alpha-2-HS-glycoprotein (fetuin), vitamin D-binding protein, splicing factor (SRp20), ribosomal protein S2 (Rps2), Ribosomal protein L29, T-cell differentiation protein 2 (Mal2), 5,10-methenyltetrahydrofolate synthetase (Mthfs), alpha-1-inhibitor III, argininosuccinate synthetase (Ass), afamin (Afm), and CD81. Hrs is a gene producing a protein which is a substrate of Hepatocyte growth factor-regulated tyrosine kinase (MET) (98). The other proteins identified are either circulating in the plasma (fetuin, afamin), located in the cytosol (Hrs, vitamin D binding protein), or having no apparent connection in location and function. Since GPC3 is a cell surface protein, we decided to focus on the only potentially interacting protein that was also located on the plasma membrane.

CD81 (also known as TAPA-1, acronym for Target of Anti-proliferative Antibody 1) is a cell surface tetraspanin and reported to be involved in a variety of biologic responses including inhibition of growth and proliferation (99). In the liver, previous research revealed that CD81 interacts with HCV glycoprotein E2, assisting with HCV entry into hepatocytes(100). Still, the overall role of CD81 in liver growth regulation has not been previously investigated. As a first step, we assayed CD81 RNA and protein levels during liver regeneration. The results of semi-quantitative RT-PCR and western blotting showed that RNA and protein levels of CD81 start increasing from day 2 (Fig.11A, B), which corresponds with changes of GPC3.

2.2.5 GPC3 Co-immunoprecipitates with CD81

The yeast two-hybrid assay suggested that CD81 interacts with GPC3. To further test this finding, we performed a co-immunoprecipitation assay. Total protein was extracted from frozen normal rat liver, and CD81 was immunoprecipitated with anti-CD81 antibody, or hamster IgG as a binding control. The immunoprecipitated material was then probed for the presence of GPC3 using an anti-GPC3 polyclonal antibody. Fig.14 shows that the 89 kDa band of GPC3 co-immunoprecipitates with CD81, but not the control IgG.

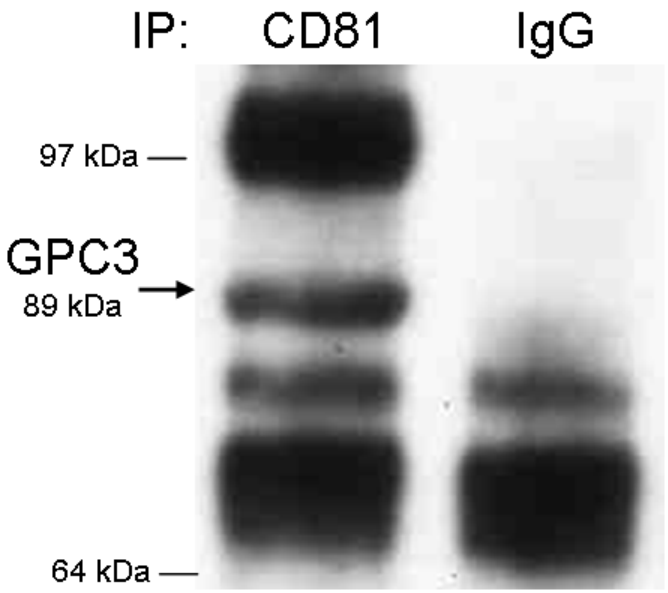

Figure 14. Co-Immunoprecipitation of CD81 and GPC3. The rat liver lysates without heparitinase treatment were incubated with anti-CD81 monoclonal antibody or control IgG, followed by precipitation with agarose A/G plus beads. Precipitates were separated by western blotting and probed with anti-GPC3 rabbit polyclonal antibody. Arrowhead indicates the 89 kDa GPC3 protein.

2.2.6 Localization of GPC3 and CD81 in Hepatic Tissue by Immunofluorescence

To further study the intracellular localization of GPC3 and CD81 in the liver, co-immunofluorescence was performed. Frozen sections of liver after PHx were double labeled with primary antibodies against GPC3 and CD81, and visualized using confocal microscope to determine the localization of both proteins. Our results showed that both GPC3 and CD81 localize on cell membranes during liver regeneration. At day 2 after PHx, based on cell morphology, strong co-localization appeared on hepatocyte plasma membranes while at day 6, the co-localization signal appeared mainly along the sinusoids (Fig.15). It has been previously reported (68) that during the rat liver regeneration, rat hepatocytes start proliferating first and finish proliferation around day 2, followed by the proliferation of other cell types. The whole process lasts about 5 to 7 days. Therefore, the co-localization of GPC3 and CD81 at day 2 coincides with the termination of hepatocyte proliferation, while the co-localization on non-hepatocyte cell types at day 6 likely reflects the cessation of proliferation of non-parenchymal cell types. Western blotting results (Fig.11B) also revealed that there was an increase of GPC3 at day 2 and CD81 at day 1 after PHx, followed by another peak around day 5.

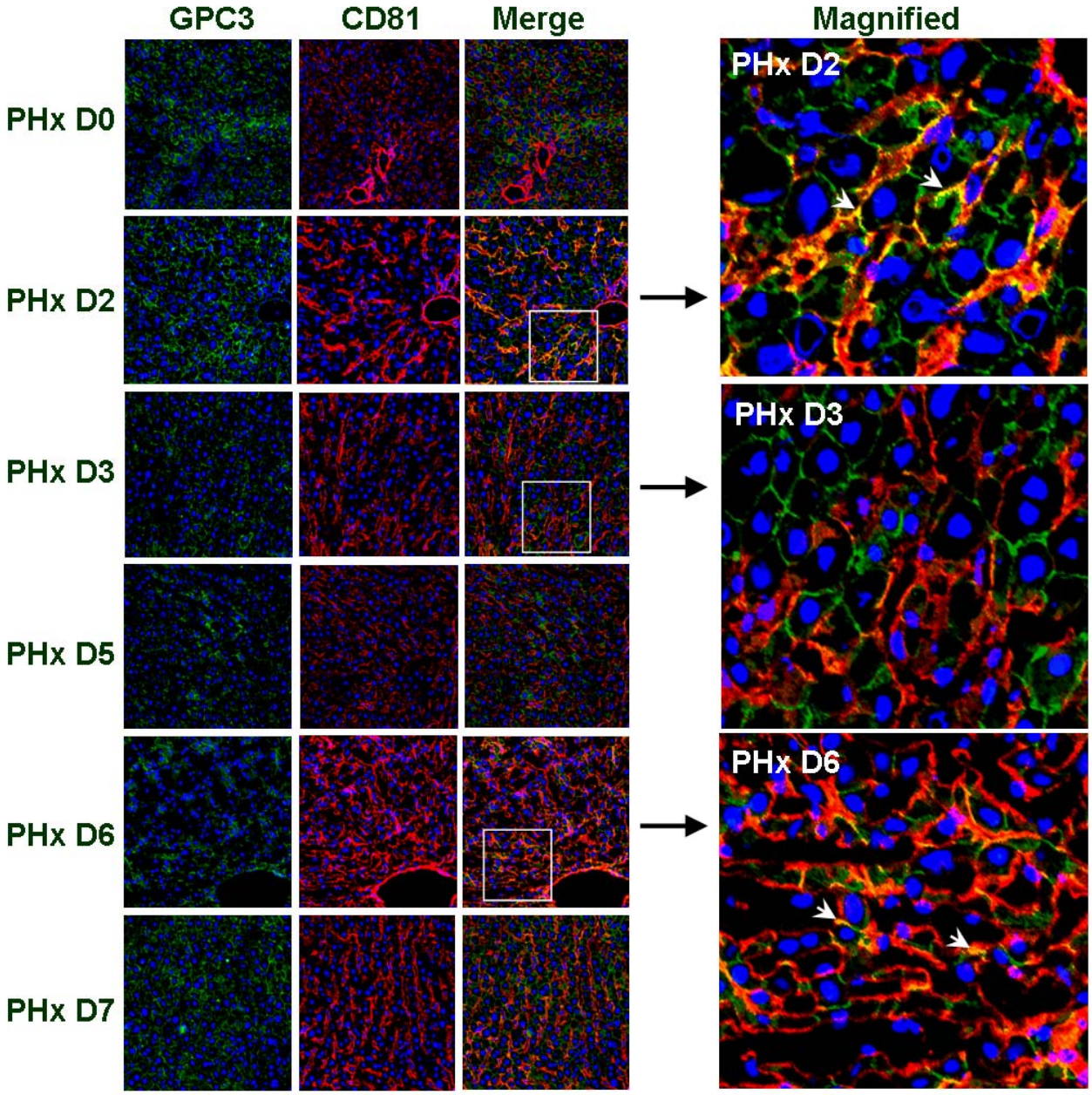

Figure 15. Immunofluorescence Analysis of GPC3 and CD81 Expression in Rat Liver Regeneration Process. Olympus Fluoview 500 Confocal Microscope was used to visualize the images and the original magnification was 200X. GPC3 (green), CD81 (red) and DRAQ5 nuclear staining (blue) are shown. Co-localization signals at day 2 and 6 after PHx are shown in the merged images (see white arrowheads in the magnified image).

2.3 DISCUSSION

In this study, we showed that GPC3 mRNA and protein increase in a time frame which coincides with the termination of proliferative activities of either hepatocytes (day 2 after PHx and Day 8-12 in culture) or non-parenchymal cells (Day 5-6 after PHx). These results and the previous reports about the GPC3 mutation in SGBS and organomegaly in GPC3 knock-out mice are consistent with our hypothesis that GPC3 plays an overall growth inhibitory role, at least in liver regeneration and hepatocyte proliferation. The studies with patients suffering from SBG syndrome also suggest that GPC3 is involved in regulating the growth of mesenchymal tissues, including muscle and bone etc. This correlates with the changes observed with GPC3 at Day 5 and thereafter following PHx, which involve proliferation of non-hepatocytic cells types, such as stellate cells and endothelial cells (68).

The yeast two-hybrid assay suggests that GPC3 interacts with CD81 which is a cell membrane tetraspanin, a finding which we validated by co-immunoprecipitation. Further study showed that CD81 mRNA and protein increase in grossly the same time frame after PHx. Co-immunofluorescence results show that GPC3 and CD81 co-localize at day 2 and day 6 after PHx, indicating an important regulator interaction between the two proteins. At day 2 after PHx, strong signal of co-localization of GPC3 and CD81 appeared mainly on the cell membrane of hepatocytes. This coincides with the termination of hepatocyte proliferation. At day 6 after PHx, when all the other cells are finishing proliferation and arrangement, the co-localization signal appeared mainly along the sinusoids. These results suggest a potential regulatory role involving

an interaction of CD81 and GPC3 at times in which separate cellular populations in the liver (hepatocytes at Day 2 and non-parenchymal cells in Days 5-7) cease to proliferate.

In view of our results and the studies with SBGS in humans and knock-out mice, the high levels of GPC3 observed in human HCC (18) are puzzling. We also observed, in rat liver tumors generated by DEN, that different levels of GPC3, some absent and some strikingly elevated, were seen (data not shown) (18). The elevated expression of GPC3 seen in liver cancer may reflect the fact that the neoplastic hepatocytes attempt to raise their level of GPC3 as a built-in hepatocyte feedback aimed to stop their proliferation. HCC cells, however, have lost their capacity to respond to this growth termination signal. Recent studies have also shown that GPC3 is elevated in hepatic progenitor cells (oval cells) in situations when liver regeneration is stimulated and hepatocyte proliferation is blocked (101). It is also possible that in those studies GPC3 may act as a growth regulator for hepatic progenitor cells.

In general, GPC3 has been reported to interfere with different pathways and growth factors, and it has tissue and stage specific roles in development and tumor growth (30). There are several glypicans and syndecans which could interact with growth regulatory pathways. It has been reported that HSPGs interact with FGFs, BMPs, Wnt pathway, et al (38,47). And those HSPGs could act as co-receptors, which regulate the binding affinity of these growth factors to their receptors (102). Therefore, it would be very interesting to investigate the role of GPC3 with other heparan sulfate proteoglycans during liver regeneration and hepatocyte growth and proliferation.

The interaction of GPC3 and CD81 is intriguing. One could speculate that the negative regulatory effects of GPC3 may be mediated via CD81. Since the latter is known to be a major portal of entry of HCV into hepatocytes (100), the finding raises the possibility that HCV interacting with CD81 disrupts a major growth regulatory pathway for hepatocytes. In view of the well documented but poorly understood high frequency, induction of hepatocellular carcinomas by HCV, this possibility is worthy of further exploration.

3.0 SUPPRESSION OF LIVER REGENERATION AND HEPATOCYTE PROLIFERATION IN GLYPICAN 3 HEPATOCYTE-TARGETED TRANSGENIC MICE

To further study the role and mode of action GPC3 during the liver regeneration process, we generated GPC3 transgenic (TG) mice under the control of the mouse albumin promoter/enhancer, in order to over-express GPC3 specifically in mouse hepatocytes. The GPC3 TG mice appeared phenotypically normal and were indistinguishable from their non-transgenic littermates. Further investigation by western blotting and immunofluoresence staining revealed an up-regulation in GPC3 levels in the resting liver of these TG mice. We also found that after 2/3 PHx, liver regeneration and hepatocyte proliferation was suppressed in these TG mice, as shown by our assessment of hepatocyte proliferation and the liver weight growth curve. Gene array analyses demonstrated an altered gene expression profile in the TG mice compared with their wild-type (WT) littermates. A comparison of gene expression profiles at various time points after PHx revealed a panel of cell cycle related genes and growth arrest genes there were either up- or down-regulated. Western blotting confirmed the changes of key factors in specific pathways. The overall findings suggest that GPC3 is indeed a suppressor of hepatocyte growth

and that it may play a role in regulation of the processes resulting in termination of liver regeneration.

3.1 MATERIALS AND METHODS

3.1.1 Transgenic (TG) Construct and Production of GPC3 TG Mice

A 1.8 kb mouse GPC3 insert containing the entire coding region was cloned from mouse liver cDNA library and inserted into the *Bam*HI site of an albumin promoter-driven expression vector kindly provided by Dr R Palmiter (University of Washington, USA). This transgene construct was used to generate transgenic mice using the FVB mouse strain (Taconic, NY, USA) by established methodology (103). Transgenic mice were identified by PCR using a forward primer located in the albumin promoter region: CTGCACACAGATCACCTTT and a reverse primer located within GPC3 exon 2: GCCGTGCTGTTAGTTGGTATTTTTCT. Transgenic mice were further confirmed by Southern blotting of *BSRG*I digested mouse tail genomic DNA using a ^{32}P-labeled 288 bp GPC3 cDNA probe using standard hybridization conditions (104). One of three transgenic lines produced was utilized for this study, based upon its high GPC3 transgene expression. Heterozygote mice were propagated by breeding with each other to produce homozygote carriers. WT FVB mice were used as controls. All animals were housed in the animal facility of the University of Pittsburgh in accordance with the guidelines of the Institutional Animal Use and Care Committee of the University of Pittsburgh.

3.1.2 Mouse PHx Model

All mice were housed with a 12-h light/dark schedule and allowed access to food and water ad libitum. Isoflurane inhalation (Baxter, IL, USA) was used to anaesthetize animals. In the mouse 2/3 PHx model, the median and left lobes were resected from TG and WT male mice between 20 and 30 weeks of age. The remaining liver lobes were obtained from defined time points after PHx as: day 2 (2d), 4d and 6d for morphological, immunohistochemical and molecular analysis. All procedures performed on these mice were approved under the IACUC protocol and conducted according to National Institute of Health guidelines.

For each time point after PHx, the remaining liver weight was recorded. A portion of the liver tissue was fixed in 10% formalin solution for 48 hours and embedded in paraffin, or placed in Tissue-Tek OCT embedding compound and frozen on dry ice. The rest of the liver samples were promptly frozen in liquid nitrogen and stored at -80°C. For some animals, hepatocytes and NPC cells were isolated by an adaptation of Seglen's calcium 2-step collagenase perfusion technique (95) as previously described from our laboratory (73). All numerical results are expressed as mean ± standard error (SE).

3.1.3 RNA Extraction and Semi-Quantitative RT-PCR

RNA was extracted from frozen liver tissues with Trizol (Invitrogen, CA, USA) according to the manufacturer's instructions. 5 ug of RNA was reverse-transcribed to complementary DNA (cDNA) and semi-quantitative RT-PCR was performed as described in our previous paper (105). The primer sequences used to perform PCR are: mGPC3-Forward: GCACGGCTGAACATGGA ACAACTGCTC; mGPC3-Reverse: GGGGTAGTTATTCTTGAACATGGCGTTGGT; mCD81-Forward: CGCGGTACCATGGGGGTGGAGGGCTGCAC; mCD81-Reverse: CCGGAATTCT CAGTACACGGAGCTGTTCCGG. Porphobilinogen deaminase (PBGD, NM_013551.2) primers were used as the control: mPBGD-Forward: ATGTCCGGTAACGGCGGC; mPBGD-Reverse: CAAGGCTTTCAGCATCGCCACCA. The signal intensity was quantitated using ImageJ software and normalized to PBGD control.

3.1.4 Protein Extraction and Western Blotting

Whole liver protein extract was obtained by homogenizing frozen liver tissue in RIPA buffer (50mM Tris-HCl, pH 7.4, 150mM NaCl, 0.1% SDS) supplemented with proteinase inhibitors. Nucleus protein was extracted using NE-PER Nuclear and Cytoplasmic Extraction Reagent Kit (Thermo Scientific, IL, USA) according to the manufacturer's protocol. Protein samples (20 ug) were resolved on 4% to 12% NuPage Bis-Tris gels (Invitrogen, CA, USA) and western blotting was processed as described in our previous paper (105). A minimal of three liver samples per time point were pooled for western blotting, and the signal intensity of each protein band was

quantitated using National Institutes of Health ImageJ software. β-actin was used as the loading control for western blotting with total liver protein lysates (Fig.16B,C,D), while ponceau staining of each protein column was quantitated as the loading control for western blots using nucleus or cytoplasm proteins (Fig.19). The primary antibodies used in this study were: GPC3 rabbit antibody (Aviva, CA, USA); CD81 hamster antibody (GeneTex, TX, USA); Cyclin D1 rabbit antibody (NeoMarkers, CA, USA); Proliferating Cell Nuclear Antigen (PCNA) mouse antibody (Santa Cruz, CA, USA); yes-associated protein (YAP) rabbit antibody (Cell Signaling, MA, USA); phosphorylated YAP rabbit antibody (Cell Signaling, MA, USA); Early growth response factor 1 (Egr1) mouse antibody (Abcam, MA, USA); c-Myc rabbit antibody (Santa Cruz, CA, USA); C/EBPα rabbit antibody (Santa Cruz, CA, USA);. C/EBPβ rabbit antibody (Santa Cruz, CA, USA) and runt related transcription factor 3 (Runx3) rabbit antibody (Abcam, MA, USA).

3.1.5 Co-immunofluoresence

Frozen rat liver sections (5 μM) were fixed in ice cold 100% acetone and co-stained successively with primary antibodies against GPC3 (Aviva, CA, USA) and CD81 (GeneTex, TX, USA) as described in our previous study (105). Sections were counterstained with the nuclear DNA probe DRAQ5 (Biostatus Limited, UK). Images were visualized using a Nikon Eclipse confocol fluorescent microscope.

3.1.6 Immunohistochemistry

Liver paraffin sections from each sample were cut at 5 μM and stained with proliferation marker Ki67 rabbit antibody (ThermoFisher Scientific, MA, USA) using the avidin-biotin-peroxidase complex technique (Vectastain ABC kit and DAB peroxidase substrate kit, Vector Laboratories, CA, USA). The tissue was counterstained with hematoxylin and Eosin (H&E). The staining was visualized using Axiovert 40 CFL inverted microscope (Carl Zeiss MicroImaging, NY, USA) and statistically analyzed. Average hepatocyte proliferation rate was demonstrated by the percentage of Ki67-positive hepatocytes in the total number of hepatocytes in 13 random selected fields taken with a 20X magnification for each group of mice.

3.1.7 Gene Array Analysis

Multiple frozen liver samples from each time point for GPC3 TG mice or WT mice were pooled and RNA was extracted for microarray hybridization. Double stranded cDNA was synthesized from total RNA and used as the template for *in vitro* transcription to generate biotin-labeled cRNA according to manufacturer's instructions. 8 μg of the labeled cRNA from each sample was fragmented and hybridized to the Mouse Genome 430 2.0 GeneChip array (Affymetrix, CA, USA) and the signal was amplified by the biotin-avidin-phycoerythirn technique. Affymetrix scanner 3000 7G and Genechip Operating software 3.2 (Affymetrix, CA, USA) were used to scan the images and convert intensity to a numerical format representing an average difference value for each probe.

3.2 RESULTS

3.2.1 Generation of TG Mice Over-expressing GPC3 in the Liver

To generate GPC3 transgenic mice, we designed and cloned a transgenic expression construct containing the 1.8 kb coding region of GPC3 cDNA under the transcriptional control of the mouse albumin promoter/enhancer (Fig. 16A). The insertion of the GPC3 transgene was confirmed by PCR and Southern blotting in GPC3 TG mice (data not shown). To examine the changes in mRNA and protein levels of GPC3, semi-quantitative RT-PCR and western blotting were utilized in livers from TG and WT mice, with a minimal of three mice per time point examined. As expected, there was increased GPC3 protein in TG mice at day 0 and at day 2 after PHx compared with their non-transgenic littermates (Fig. 16B,D). GPC3 protein increased at 4 days after PHx in WT mice, as we had previously described (105), while in TG mice it remained essentially unchanged (Fig. 16B). Of interest, CD81 protein levels were also significantly up-regulated in GPC3 TG mice, with a downtrend during the liver regeneration process (Fig. 16C,D).

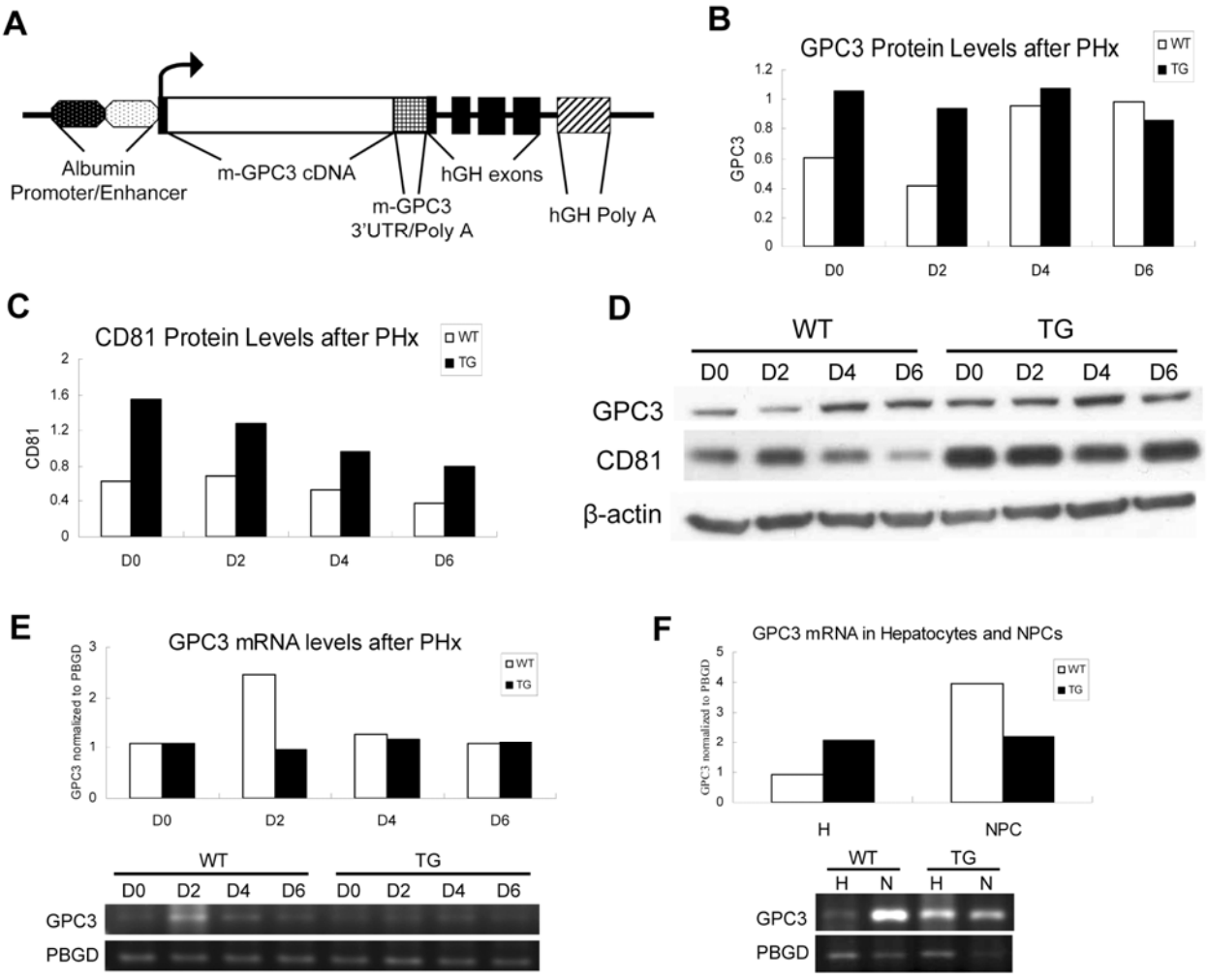

Figure 16. The Transgene Construct and Expression Levels of GPC3 Transgene. (A) Schematic representation of the GPC3 transgene consisting of the 1.8 kb mouse GPC3 cDNA (open box) with GPC3 3'UTR/Poly A (square mesh box) inserted into the first exon of the human growth hormone gene (black boxes) controlled by the mouse albumin enhancer/promoter (dotted ovals), and possessing a human growth hormone Poly A site (cross box). Western blotting results showed that GPC3 (B) and CD81 (C) protein levels, normalized by β-actin, were up-regulated in TG mice. TG: GPC3 transgenic mice. WT: FVB wild-type mice. (D) Original western blots showing GPC3 and CD81 levels during liver regeneration process in WT and TG mice. (E) Semi-quantitative RT-PCR of GPC3 results normalized to control PBGD expression and quantitated using ImageJ software. No significant changes in GPC3 mRNA levels were observed in total liver tissue in TG and WT mice. (F) Semi-quantitative RT-PCR analysis of GPC3 expression in hepatocytes and NPCs in WT and TG mice. H: hepatocytes. NPC: non-parenchymal cells.

Semi-quantitative RT-PCR results were quantitated using ImageJ software and showed no obvious change in GPC3 gene expression between TG and WT mice, after normalization to PBGD expression, in the total liver extracts (Fig. 16E). This may be due to the fact that only non-parenchymal cells (NPC) express significant levels of GPC3 in the WT mice, whereas in the transgenic mice both hepatocytes and NPC express GPC3 at moderate levels (Fig. 16F). In contrast, using immunofluorescence, we saw an increase in GPC3 protein on hepatocyte membranes as well as in cytoplasm of TG mice compared with their WT littermates (Fig. 17A).

3.2.2 Growth Suppression after PHx in GPC3 TG Mice

To further study the function and role of GPC3 *in vivo*, mouse 2/3 PHx was performed in both GPC3 TG and WT male mice, and liver tissue samples were collected at days 2, 4 and 6. Liver weight was assessed by normalizing to the day 0 total liver weight in each group. The data are presented in Figure 18A. There was no significant difference of the total (pre-hepatectomy) liver weight at day 0 when comparing TG and WT mice (data not shown). At day 6 after PHx, the liver weight of GPC3 TG mice was significantly lower than that of WT mice (Fig. 18A). Ki67 immunohistochemistry results showed that in WT mice there was abundant hepatocyte proliferation at 2 days after PHx, as demonstrated by the percentage of Ki67 positive nuclei. In GPC3 TG mice, hepatocyte proliferation was significantly suppressed at day 2 post-PHx (Fig.17B,18B), with no significant differences at days 4 and 6 compared with WT.

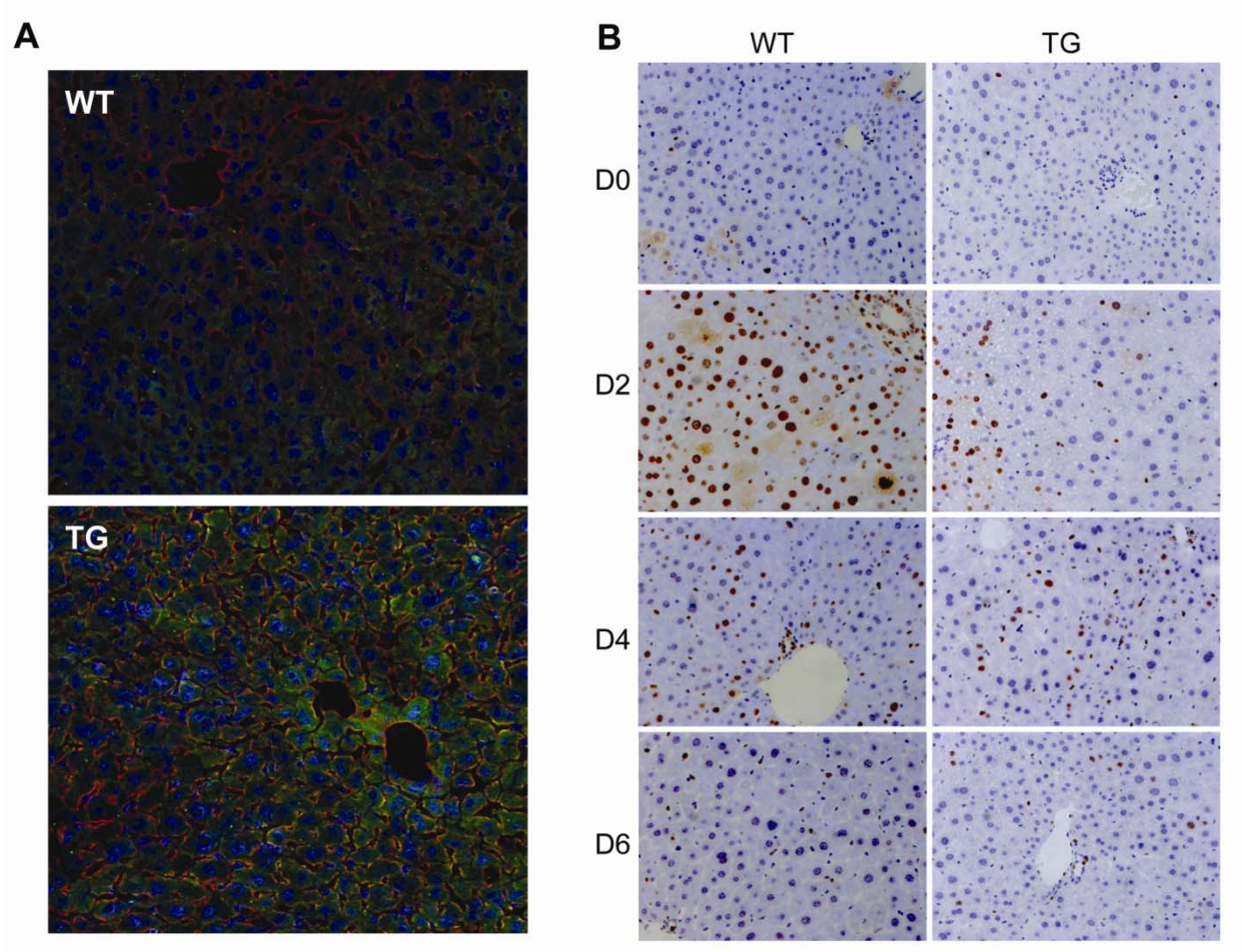

Figure 17. Immunofluoresence Staining of GPC3 and Immunohistochemistry Staining of Ki67 in TG and WT Mice. (A) Olympus Fluoview 500 Confocal Microscope was used to visualize the images of the liver in TG and WT mice. GPC3 (green), CD81 (red) and DRAQ5 nuclear staining (blue) are shown in the merged images with a magnification of 200X. TG mice showed a significant increased level of GPC3. (B) Immunohistochemistry staining and Ki67 (brown), a proliferation marker, in paraffin sections of TG and WT mice livers after PHx. The Ki67 positive rate was suppressed in TG mice at day 2 after PHx compared with WT mice.

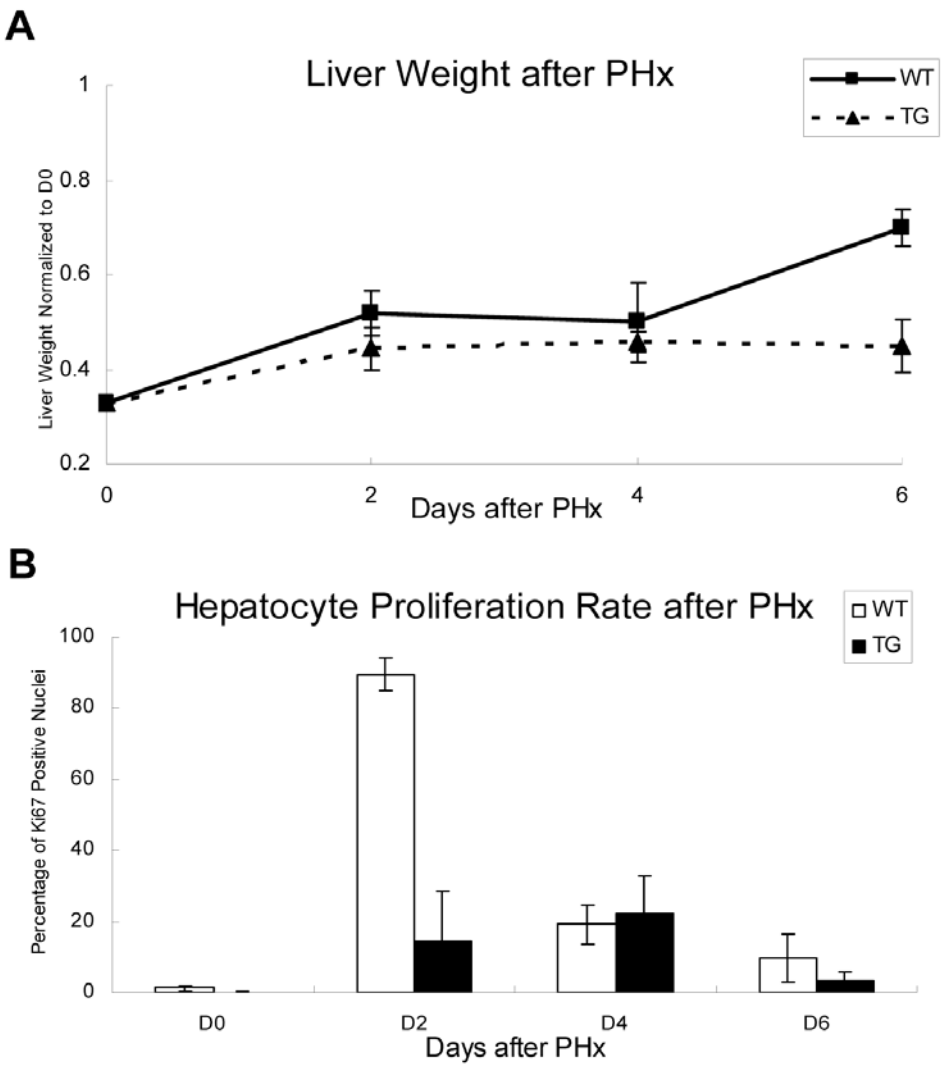

Figure 18. Suppression of Liver Regeneration and Hepatocyte Proliferation in GPC3 TG Mice. (A) Statistic analysis of liver weight of TG and WT mice after PHx, normalized to day 0 total (pre-hepatectomy) liver weight. D0 in the graph represents the remaining liver weight after PHx, which is 1/3 of the total liver weight. There was no significant difference in the pre-hepatectomy liver weights at day 0 between TG and WT mice. (B) Positive Ki67 positive staining in hepatocytes of TG and WT mice after PHx. A significant decrease in Ki67 positive rate was observed in TG mice at day 2 after PHx.

3.2.3 Gene Expression Profile Alteration in Unoperated TG Mice

Microarray analysis was used to investigate the expression profile and transcriptional regulation in liver tissues of TG and WT mice under normal conditions (unoperated mice). The Mouse Genome 430 2.0 GeneChip array is a single array analyzing the expression level of over 39,000 transcripts and variants, including over 34,000 well-characterized mouse genes (Affymetrix, CA, USA). Direct comparison between TG mice and WT mice expression patterns revealed 44 genes up-regulated and 58 genes down-regulated in TG with > 1.5 fold change (Appendix Table 2). Among the most interesting were *Runx3* (Runt related transcription factor 3, up by 7.6-fold), *Jak3* (Janus kinase 3, up by 6.4-fold), *Dbp* (D site Albumin promoter binding protein, up by 4-fold), *Gabaar* (GABA-A receptor, up by 2.9-fold), *Wnt7b* (Wingless-related MMTV integration site 7B, up by 2.8-fold) and *Egfr* (epidermal growth factor receptor, up by 1.6-fold). *Gpc3* and *Cd81* genes were both up-regulated by 1.5-fold in TG mice. Most strongly down-regulated genes were *Igfbp1* (insulin-like growth factor binding protein 1, down by 8.4-fold), *Rab2* (RAS oncogene family, down by 5.6-fold), *Egr1* (Early growth response 1, down by 5.3-fold), *Tgfb1* (Transforming growth factor beta type I, down by 3.1-fold), *Ndl* (Nodal, down by 1.8-fold), *Catnb* (beta catenin, down by 1.7-fold) and *Yap* (Yes-associated protein, down by 1.4-fold) in GPC3 TG mice. A complete list of genes showing either up- or down-regulation in expression of TG mice can be found in Appendix Table 2. Some of these genes are involved in multiple regulatory pathways, with their changes in expression presumably affected by the over-expression of the GPC3 transgene in mouse hepatocytes.

3.2.4 Gene Expression Profile Altered after PHx in TG Mice

A comparison of expression profiles between TG mice and WT mice after PHx also indicated dysregulation of many genes in GPC3 TG mice during liver regeneration. A panel of important genes known to be involved in hepatocyte cell cycle and growth arrest was examined and analyzed at 2 days after PHx in TG mice compared with their WT littermates, when the biggest suppression of hepatocyte proliferation occurred (Appendix Table 3). Some cell cycle related genes were observed to be down-regulated in TG mice at day 2 post-PHx, such as *Ccna1* (Cyclin A1, by 7.6-fold), *Ccnm1* (Cyclin M1, by 5.4-fold), *Ccnd1* (Cyclin D1, by 1.4-fold), *Ccne2* (Cyclin E2, by 1.7-fold), and *Gas1* (Growth arrest specific 1, by 1.7-fold). The up-regulated genes after PHx in TG mice were: *Runx3* (by 8-fold), *Gadd45b* (Growth arrest and DNA-damage-inducible 45 beta, by 3.9-fold), *Fgf14* (Fibroblast growth factor 14, by 2-fold) and *Tgfb1* (by 1.6-fold). A series of *Cdks* (Cyclin-dependent kinases), *Ccns* (Cyclins) as well as *Igfbps* (Insulin-like growth factor binding proteins) was also observed to be altered at day 2 after PHx in TG mice. Some other important genes that are related to growth and proliferation with less significant changes in TG mice, if any, are also listed for reference (Appendix Table 3).

3.2.5 Growth Related Protein Differences after PHx between GPC3 TG and WT Mice

Gene array results revealed a panel of cell cycle related and growth related genes, the expression of which is altered in GPC3 TG mice after PHx compared to their WT littermates. Western

blotting was performed to further investigate the protein levels of some of these genes (Fig. 19). For each time point, liver samples from a minimum of three mice were pooled and the nuclear and the cytoplasm proteins were separated for western blotting. Prior to PHx, there was an increase in the protein levels of c-Myc, Egr1, C/EBPα and Runx3 in TG mice compared with WT. Except for Egr1, these findings correlate with the changes seen for these proteins by gene array analyses. After PHx a decrease in levels of some of the proteins in the nucleus was observed at day 2 in GPC3 TG mice, such as Cyclin D1, PCNA, c-Myc and YAP. There was also increased phosphorylated YAP (p-YAP) protein in cytoplasm, which is the inactive form of YAP. C/EBPβ level was increased at day 4 and day 6 after PHx in TG mice. These results coincided with the suppression of liver regeneration and hepatocyte proliferation after PHx.

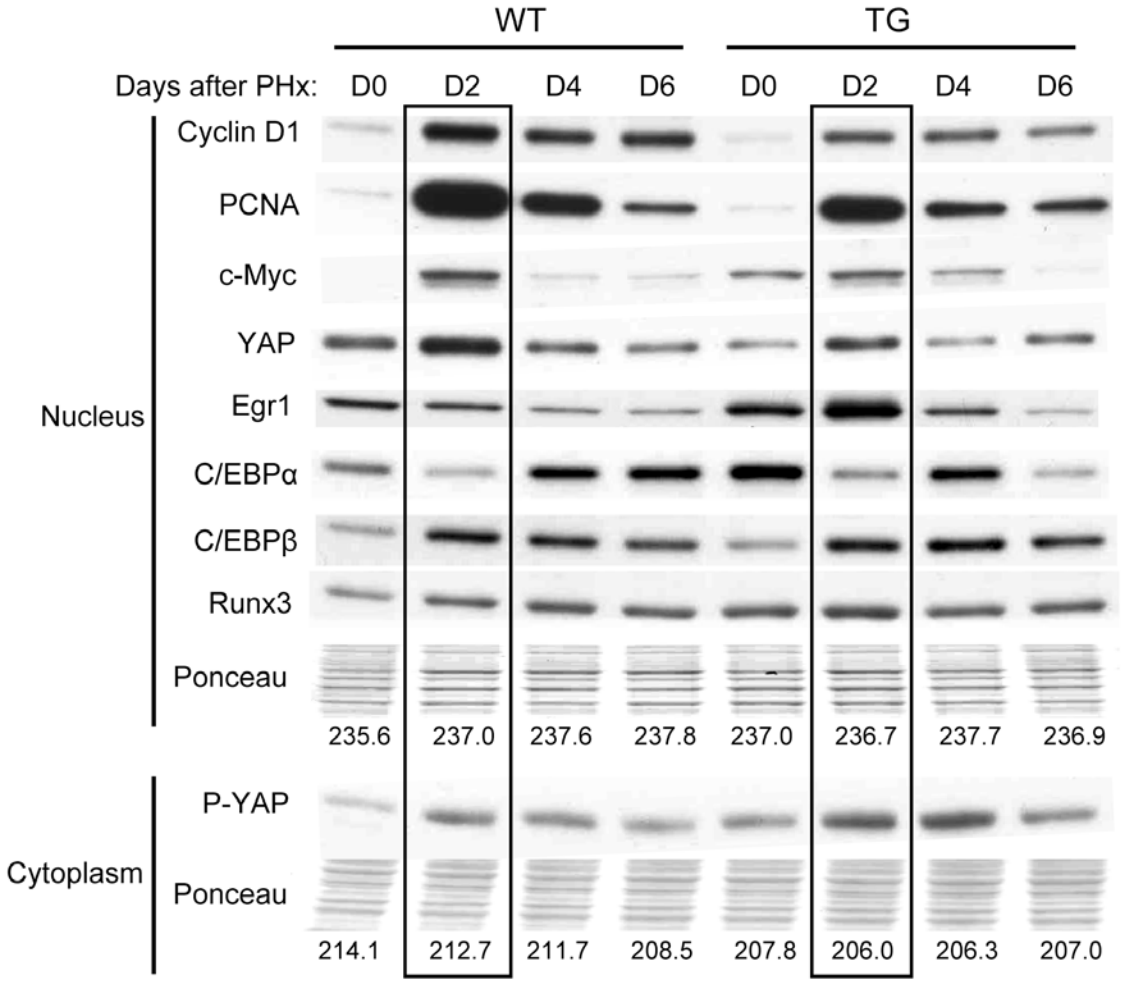

Figure 19. Western Blotting Results Showing Changes in Protein Levels of Selected Genes from GPC3 TG Mice and WT Mice during Liver Regeneration. Protein levels in the nuclei and cytoplasm of livers from GPC3 TG and WT mice were examined. Ponceau staining of each protein lane was used as loading control and the average grey value was shown below each column. The protein levels at day 2 after PHx are highlighted in TG and WT mice.

3.3 DISCUSSION

Liver regeneration is a complicated process and involves multiple factors and pathways (68). Our previous study showed that GPC3 plays an inhibitory role during rat liver regeneration and hepatocyte proliferation. The work performed in this study further suggests the effects of GPC3 on hepatocyte growth are primarily inhibitory, using our GPC3 transgenic mouse model. We generated GPC3 transgenic mice using a transgenic construct under the transcriptional control of the mouse Albumin promoter/enhancer, targeting for hepatocyte-specific expression. These TG mice showed no apparent phenotypic difference compared to their non-TG littermates, but further investigation revealed an up-regulation in GPC3 protein levels in the liver of these TG mice.

To study the effect of GPC3 transgene over-expression on liver regeneration, we compared the liver weight, normalized to day 0, between TG and WT mice at specific time points after PHx for each group. Male mice at the age of 20-30 weeks, in which the hepatocyte polyploidization process becomes relatively steady, were selected to investigate the liver regeneration process (106,107). A suppression of liver growth was observed on day 6 after PHx in TG mice. Immunohistochemistry results revealed a significant suppression of the proliferation rate in TG mice at 2 days after PHx, when there is a peak of hepatocyte proliferation in WT mice. The suppression of liver growth and hepatocyte proliferation after PHx coincided well with the over-expression of the GPC3 transgene and the up-regulated GPC3 protein levels in these TG mice. This also abides with our previous hypothesis that GPC3 plays a negative regulatory role in the

liver, since GPC3 up-regulation correlated with suppression of liver regeneration and hepatocyte proliferation.

It is reported that GPC3 is involved in several pathways during development and tumorigenesis, and acts as potential co-receptor for many growth factors (30). To study the pathways that might be altered and affected by over-expression of the GPC3 transgene in the liver, we examined and compared the expression profile of TG mice and WT mice at rest and during the liver regeneration process. Our gene array data revealed alterations in the expression of over 100 genes in GPC3 TG mice, with GPC3 expression itself up-regulated by 1.5 fold. Western blotting and immunofluoresence showed an increase of GPC3 protein levels in the livers of TG mice. But interestingly, the GPC3 transgene expression at the mRNA level was not as high as expected after PHx possibly, because the albumin promoter/enhancer is known to be down-regulated slightly during liver regeneration (108,109). Examination of GPC3 expression in whole liver showed no obvious change between TG and WT mice. This might be due to a masking effect of GPC3 expression from NPCs which was relatively high in both TG and WT mice. In WT mice, the GPC3 protein levels were increased in the liver after PHx, while in TG mice with overall higher GPC3 levels than WT mice, there was a slight decrease, if any, at 2 and 6 days post-PHx. This lack of increase might be due to the down-regulation of the Albumin promoter, which is controlling the GPC3 transgene, in the early stages of liver regeneration (109-111). Previous studies showed that a decrease of nuclear factors C/EBPα and Dbp (108) and an increase of C/EBPβ (109) were involved in the down-regulation of Albumin expression during liver regeneration. Our western blotting results confirmed the down-regulation of C/EBPα and up-regulation of C/EBPβ after PHx in GPC3 TG mice (Fig. 19) In gene array analysis, we also observed an 11.5-fold decrease in the expression of *Dbp* at 2 days after PHx in the TG mice (data

not shown). The changes of these nuclear factors may lead to down-regulation of the Albumin promoter in TG mice, which may explain the decrease of GPC3 protein levels at day 2 and day 6 after PHx.

The suppression of regeneration seen in this study corresponds well with some of the changes noted in the TG mice prior to PHx. GABA A receptor is over expressed by 2.9-fold. Previous studies have also shown that GABA and its receptor also have inhibitory effects on liver regeneration (112). Runx3, another over-expressed gene in the TG mice, is associated with suppression of Notch signaling events in the liver (113). NICD, the Notch intracellular domain, is associated with stimulation of hepatocyte proliferation during liver regeneration (82). The role of Wnt7b is not clear. There is minimal expression of Wnt7 in normal mouse liver and, if any, it is expressed in NPC cells (48). Surprisingly, there is over-expression of EGFR, a major mitogenic receptor for hepatocytes (114). This may reflect a compensatory effect associated with a prolonged increase of the growth-inhibitory GPC3 in the liver of the TG mice. Although the expression of *Egr1* is down-regulated by 5.3-fold, there are enhanced protein levels of Egr1 in TG mice, which might be due to the effect of microRNAs or the protein stability. The enhanced protein level of Egr1 may also correlate with the observed effects on liver regeneration since Egr1 is known to suppress expression of the HGF receptor (115). The changes associated with cell cycle related genes after PHx are easier to correlate with the observed suppression of liver regeneration, especially in relation to cyclin A and D1, well known to be associated with entry of hepatocytes into S-phase of the cycle (116). The observed increase in C/EBPα also relates to the overall suppression of regeneration, since C/EBPα is known to decrease following PHx (117). Equally important is the observed decrease in YAP nuclear levels in TG mice, associated with an

increase in cytoplasmic levels of p-YAP. YAP is known to correlate with hepatocyte growth and adjustment of liver size (118,119). Phosphorylation of YAP is associated with export from the nucleus to the cytoplasm and suppression of its effects on the regulation of growth related genes (119).

The results of our current work further extend the evidence that GPC3 has overall growth-suppressive effects on hepatocytes. GPC3, however, is greatly elevated in human hepatocellular carcinoma (18). One can rationalize that the increased expression of GPC3 in liver cancer reflects an existing gene expression algorithm by which proliferating hepatocytes regulate their growth, as in liver regeneration. GPC3, however, is also reported to be elevated in liver progenitor (oval cell) populations (101), a cell population which is not neoplastic. Despite all the accumulated literature on growth regulation by GPC3, its mechanisms of action remain elusive. It is associated with CD81, as shown in this work. The latter also has growth regulatory effects in specific cell populations (105). We published that there is enhanced association between GPC3 and CD81 after PHx (105). This may result in suppression of CD81 signaling, a protein of which little is known. Since not much is known about the pathways involved in termination of liver regeneration, further studies should focus on fully understanding the signaling pathways associated with the effects of GPC3 in normal liver, in order to better conceptualize its high levels of expression in liver neoplasia.

4.0 GENERAL DISCUSSION AND FUTURE DIRECTIONS

GPC3 is a GPI-anchored cell-surface heparin sulfate proteoglycan which plays important roles during embryogenesis and organogenesis as well as tumorigenesis. Despite all the accumulated literature on growth regulation and potential signaling pathways of GPC3, its mechanism of action is still not well characterized. By studying its role and mechanisms during liver regeneration process, we hope to gain insights into the functional pathway and regulation of GPC3 in different circumstances, and to better understand the regulatory mechanism of the termination of liver regeneration.

In order to investigate the role and function of GPC3 in the liver, we used 2/3 partial hepatectomy model in rats and hepatocyte-targeted transgenic mice, in which the liver regenerates through proliferation of hepatocytes and NPCs with no massive necrosis or acute inflammation associated. We also applied yeast two-hybrid assay and microarray analysis to study the potential factors involved in GPC3 pathways. Further study of GPC3 function, regulation mechanism as well as signaling pathways will be significant for better understanding the malfunction of the liver regeneration and tumorigenesis.

4.1 SUMMARY

We first studied the role of GPC3 in rat model of liver regeneration after 2/3 PHx in which hepatocyte growth dynamics are well characterized (68). We also used rat hepatocyte primary cultures, in which we and others have characterized the hepatocyte growth cycle under the influence of HGF and EGF *in vitro* (94). The RT-PCR and western blotting results demonstrated that GPC3 mRNA and protein increase in a time frame that coincides with the termination of proliferative activities of either hepatocytes (day 2 after PHx and day 8-12 in culture) or NPCs (day 5-6 after PHx). The *in vitro* proliferation and growth curve studies showed that hepatocyte growth was promoted when GPC3 expression was blocked using antisense Morpholino oligos. These results and the previous reports about GPC3 mutation in SGBS and organomegaly in GPC3-/- mice are consistent with our hypothesis that GPC3 plays a growth inhibitory role, at least in liver regeneration and hepatocyte proliferation.

To further validate this, we generated GPC3 transgenic mice under the control of mouse albumin promoter/ enhancer to over-express GPC3 specifically in the hepatocytes. The GPC3 TG mice appeared phenotypically normal and were indistinguishable from their non-transgenic littermates. Further investigation by western blotting and immunofluoresence staining revealed an up-regulation in GPC3 levels in the liver of these TG mice. We found that after 2/3 PHx, liver regeneration and hepatocyte proliferation was suppressed in these TG mice as shown by assessment of hepatocyte proliferation and liver weight growth curve, which abided with our hypothesis that GPC3 is a negative regulator during liver regeneration.

The following pathway and mechanism studies involved yeast two-hybrid assay and gene array analysis. The yeast two-hybrid assay revealed that GPC3 interacts with CD81, a cell membrane tetraspanin, as further confirmed by co-immunofluorescence and co-immunoprecipitation studies. CD81 mRNA and protein increased in grossly the same time frame after PHx. The co-localization of GPC3 and CD81 at day 2 and 6 after PHx indicated the potential for an important regulatory interaction between the two proteins.

In addition, the gene array analysis results demonstrated a series of changes in the gene expression profiles in the GPC3 hepatocyte-targeted TG mice compared with their WT littermates. Over 100 genes were either up- or down-regulated, some of which were involved in multiple regulatory pathways. After 2/3 PHx, a panel of cell cycle related genes and some oncogenes were either up- or down-regulated, which was confirmed by western blotting. These results indicated that over-expression of GPC3 in hepatocytes altered gene expression profiles, in which potential cell cycle related proteins and pathways were involved and affected.

4.2 DISCUSSION

Our studies of GPC3 after 2/3 PHx in rats and GPC3 transgenic mice indicate that GPC3 functions as a growth inhibitor, at least in the liver, which coincides with the previous observations of organomegaly in SGBS and GPC3-/- mice (14,16). The role of GPC3 provides

an insight into the termination of the liver regeneration, which is much less understood compared to its initiation process. At the end of regeneration, liver mass is adjusted and liver histology is rearranged to restore the full function of the liver under proper regulation (68). Current study of the termination signals of regeneration has focused on TGFβ1, which is produced predominantly by stellate cells (120), and also by most carcinomas derived from hepatocytes or hepatoblasts (18). As a known suppressor of hepatocyte proliferation *in vitro* (121), TGFβ1 also suppresses production of HGF (122), suppresses urokinase and activation of HGF (92), and stimulate production of many extracellular matrix (ECM) proteins in the liver (68). However, current study shows that intact TGFβ1 pathway is not required to stop liver regeneration (123) and TGFβ1 is not a direct terminator of regeneration (68), indicating the existence of other factors that regulate the termination of the regeneration.

Previous studies have shown that the regulation and remodeling of ECM play important roles during liver regeneration, which includes a mixture and complex networking of proteins and glycosaminoglycans. One of these components is GPC3, a highly glycosylated cell-surface proteoglycan existing in the pericellular matrix of many epithelial cells including hepatocytes (2). Some of the features of GPC3, such as GPI anchor, HS side chains and globular core protein structure, provide insights into the potential interactions between GPC3 and other membrane proteins or growth factors in the ECM (1,30). Current literature has suggested that GPC3 is involved in the control of cell proliferation and/or the induction of apoptosis, and may be involved in various pathways such as FGF, BMP and Wnt pathways (38,47,51). It is possible that GPC3 regulates the termination of liver regeneration and hepatocyte proliferation by

interacting with several pathways and facilitating the ECM signaling thus altering the intracellular events in the hepatocytes and NPCs.

Our yeast two-hybrid assay results reveal that GPC3 interacts with CD81, also called TAPA1 (Target of Anti-proliferative Antibody 1), which is a cell-surface tetraspanin widely expressed and also involved in a broad range of physiological responses (99,124). CD81 is shown to co-localize with GPC3 at the termination of hepatocyte and NPC proliferation. The function of CD81 is still not well understood, but evidence has suggested that CD81 is involved in intercellular interactions and intracellular signaling regulation, protein transport, endocytosis and exocytosis, *et al* (124). Previous studies show that CD81 is associated with ECM signaling and can interact with α3β1 integrin together with CD151 thus regulating cell adhesion, cell motility and integrin-mediated pathways (125,126). Direct evidence has been found that CD81 is associate with the activation of the extracellular signal-regulated kinase1/2 (ERK1/2)/mitogen activated protein kinase (MAPK) pathway and tyrosine phosphorylation of the adapter protein Shc in liver tumor (127).

CD81, as well as other tetraspanin members, can also form homo-multimers through covalent cross-linking leading to the aggregation and formation of "tetraspanin-enriched microdomains" (TEM) (128,129). TEM is different from lipid rafts in the sensitivity to temperature, cholesterol depletion, protein palmitoylation and the basic components (128). TEM possesses considerable functional importance not only because it can interact directly with various non-tetraspanin proteins, but also due to its capacity to assemble into a heterophilic network and to recruit and

regulate different partner proteins, such as integrins, cadherins, immunoglobulin superfamily proteins, regulatory proteins, proteases, G protein-coupled receptors (GPCRs), signaling enzymes and proteoglycans (such as GPC3) (128). From this perspective, it is reasonable to speculate that GPC3 may function through binding with CD81 and affecting and regulating different factors in the dynamic TEM signaling platform.

Despite the growth suppressor role shown in our results and previous studies using SGBS and GPC3-/- mice, high levels of GPC3 expression are observed in human HCC and in rat liver tumors generated by DEN (18,58), which seems to be puzzling. The elevation of GPC3 in liver cancer may reflect an existing gene expression algorithm by which neoplastic hepatocytes attempt to raise the GPC3 level to stop their own proliferation, as a failed feedback mechanism. But the hepatocellular carcinoma cells have lost their capacity to respond to this growth termination signal, possibly due to the alterations in the signaling transduction pathways in cancers. GPC3, however, is also reported to be elevated in liver progenitor populations (oval cells) which are not neoplastic (101), in a situation when liver regeneration is stimulated and hepatocyte proliferation is blocked. It is also possible that GPC3 may regulate hepatic progenitor cells. To better understand the functions and underlying mechanisms of GPC3, it is essential to further investigate GPC3 involved signaling pathways and networks under normal conditions as well as in cancers.

Purely within the realm of speculation, it is possible that in the quiescent state of non-proliferating hepatocytes, mitogenic receptors and their ligands, and mito-inhibitory receptors

and their ligands, reside in distinct domains defined by TEMs, in such a way that hepatocytes cannot be stimulated to enter into proliferation. In the state of quiescence, TEMs are also interacting with integrins and extracellular matrix. The rearrangement of pericellular matrix and membrane domains following partial hepatectomy disrupts the TEM microdomains and allows interactions between receptors and their ligands, so that the orchestrated process of regeneration can take place. At the end of regeneration, GPC3 may be required for the reestablishment of the TEM domains and the proper sequestration of the ligand receptor families so that the quiescent state can be reestablished. This process would fail if the TEMs are severely disrupted, as in the case of many cancer cell types (130-132). In this speculative scenario, GPC3 may be a transient organizer for the establishment of the TEM membrane microdomain system. Future studies need to employ careful cell fractionation to isolate TEM microdomains and their components in different stages of hepatic regeneration, to test for this speculative hypothesis.

4.3 FUTURE DIRECTIONS

GPC3 is shown to play important and distinct regulatory roles in normal tissues and tumors. But much less is known about pathways of GPC3 as well as the termination mechanisms of the liver regeneration. Therefore, further studies should be performed to fully understand the functions, regulation mechanisms and signaling pathways associated with GPC3 in normal liver, in order to better conceptualized the high levels of GPC3 in liver neoplasia. The interaction of GPC3 and CD81 is well worth investigating to better understand the correlation between the two cell

surface proteins and the involved signaling network. It is also interested to study the effect of GPC3 on the pathways and cell growth related proteins that have been altered in GPC3 TG mice, as revealed by microarray analysis. Moreover, how GPC3 interact with and regulate ECM would be another important subject, which could provide more insights into the termination of the liver regeneration. Using the GPC3 TG mice model, one could further study the effect of GPC3 over-expression in the liver under different conditions, such as chemical-induced acute liver inflammation, liver necrosis and tumorigenesis. To understand the role of GPC3 in tumors, it is also important to study the effect and pathways of GPC in different tumor cell lines in which over-expressed or silenced GPC3 is observed. In addition, characterizing the regulation of GPC3 expression and function under different circumstances would be equally important for constructing the general picture of GPC3 during embryogenesis, organogenesis and tumorigenesis.

APPENDIX

Table 2. Selected Genes Showing Changes in Expression in GPC3 TG Mice Compared with their WT Littermates.

Gene Name	Gene Symbol	Fold Change	
Regulator of G-protein signaling 16	Rgs16	11.4	Up
Runt related transcription factor 3	Runx3	7.6	Up
Janus kinase 3	Jak3	6.4	Up
Uroplakin 2	Upk2	6.1	Up
Sphingosine kinase 2	Sphk2	5.4	Up
Cortistatin	Cort	4.8	Up
Homeobox protein NKX2-6	Nkx2-6	4.3	Up
D site albumin promoter binding protein	Dbp	4.0	Up
Nuclear receptor subfamily 1, group D, member 1	Nr1d1	3.8	Up
Tropomyosin 3, gamma	Tpm3	3.5	Up
Phospholipase D2	Pld2	3.5	Up
Very low density lipoprotein receptor	Vldlr	3.4	Up
Major urinary protein 3	Mup3	3.3	Up
Growth factor receptor bound protein 2-associated protein 2	Gab2	3.2	Up

Hyaluronidase 2	Hyal2	3.0	Up
GABA-A receptor pi subunit	Gabaar	2.9	Up
Transcription factor NFAT1-D	Nfatc2	2.8	Up
Zinc-finger protein FOG-2	Fog-2	2.8	Up
Wingless-related MMTV integration site 7B	Wnt7b	2.8	Up
Neurotrophic tyrosine kinase, receptor, type 2	Ntrk2	2.8	Up
Jun-B oncogene	Jun B	2.7	Up
Nestin	Nes	2.7	Up
Lipin 1	Lpin1	2.6	Up
Galanin receptor 3	Galr3	2.6	Up
Protein phosphatase 1, catalytic subunit, beta isoform	Ppp1cb	2.5	Up
Sphingosine kinase 2	Sphk2	2.5	Up
Cytochrome P450, steroid inducible 3a41	Cyp3a41	2.2	Up
Syndecan 3	Sdc3	1.9	Up
Bcl2-associated athanogene 1	Bag1	1.8	Up
Peroxiredoxin 4	Prdx4	1.8	Up
B-cell leukemialymphoma 6	Bcl6	1.7	Up
Cytochrome P450, 2g1	Cyp2g1	1.7	Up
Integrin alpha V	Itgav	1.7	Up
Integrin alpha 5 (fibronectin receptor alpha)	Itga5	1.7	Up
Integrin beta 7	Itgb7	1.7	Up
Integrin beta 2	Itgb2	1.7	Up
Bcl2-associated athanogene 3	Bag3	1.6	Up

Epidermal growth factor receptor	Egfr	1.6	Up
Metalloproteinase inhibitor	Timp2	1.5	Up
CD 81 antigen	Cd81	1.5	Up
Cytochrome P450, 26, retinoic acid A1	Cyp26a1	1.5	Up
BCL2-antagonistkiller 1	Bak1	1.5	Up
Bcl-associated death promoter	Bad	1.5	Up
Glypican 3	Gpc3	1.5	Up
Beta-site APP-cleaving enzyme 2	Bace2	-11.0	Down
Insulin-like growth factor binding protein 1	Igfbp1	-8.4	Down
Phospholipase D1	Pld1	-7.9	Down
A disintegrin and metalloproteinase domain 12 (meltrin alpha)	Adam12	-6.9	Down
Syntaxin 1A	Stx1a	-6.4	Down
Limitin	limitin	-6.4	Down
SH3 domain protein 2A	Sh3d2a	-6.3	Down
Metallothionein 2A	Mt2a	-6.1	Down
Tubulin, alpha 7	Tuba7	-5.8	Down
RAS oncogene family	Rab2	-5.6	Down
Suc1-associated neurotrophic factor target 2	Snt2	-5.3	Down
Early growth response 1	Egr1	-5.3	Down
HS1 binding protein 3	Hs1bp3	-5.3	Down
Procollagen, type VI, alpha 2	Col6a2	-5.3	Down
Aldehyde dehydrogenase 2	Aldh2	-5.2	Down

Dynamin-1	Dyn1	-5.0	Down
Dystonin	Dst	-5.0	Down
Brain-specific angiogenesis inhibitor 1-associated protein 2	Baiap2	-5.0	Down
Crp-ductin	Crpd	-4.7	Down
Delta-like 1 homolog	Dlk1	-4.6	Down
Eph receptor A4	Epha4	-4.4	Down
Calmodulin 3	Calm3	-3.8	Down
Regulator of G-protein signaling 4	Rgs4	-3.8	Down
Interleukin 1 receptor, type I	Il1r1	-3.7	Down
Fibroblast growth factor (acidic) intracellular binding protein	Fibp	-3.5	Down
RE1-silencing transcription factor (REST) co-repressor	Rcor	-3.5	Down
Calpain 6	Capn6	-3.5	Down
Retinol binding protein 1, cellular	Rbp1	-3.3	Down
Myosin x	Myo10	-3.3	Down
Carbonic anhydrase 2	Car2	-3.3	Down
Thioredoxin 1	Txn1	-3.2	Down
WNT1 inducible signaling pathway protein 2	Wisp2	-3.2	Down
Receptor tyrosine kinase-like orphan receptor 1	Ror1	-3.1	Down
Transforming growth factor beta type I	Tgfb1	-3.1	Down
Desmin	Des	-3.0	Down
Growth arrest specific 5	Gas5	-2.9	Down
Regulator of G-protein signaling 5	Rgs5	-2.9	Down
Syndecan 4	Sdc4	-2.8	Down

Procollagen, type IV, alpha 6	Col4a6	-2.8	Down
TRAM2	Tram2	-2.7	Down
Glutamate receptor, ionotropic, NMDA1 (zeta 1)	Grin1	-2.7	Down
Elastase	EL2	-2.6	Down
Cadherin 1	Cdh1	-2.6	Down
Calsequestrin 1	Casq1	-2.6	Down
Secreted phosphoprotein 1	Spp1	-2.6	Down
Focal adhesion kinase 1	Fak1	-2.3	Down
Cytochrome P450, 4a14	Cyp4a14	-2.0	Down
Metalloproteinase inhibitor	Timp3	-1.9	Down
A disintegrin and metalloprotease domain 4	Adam4	-1.9	Down
Cytochrome P450 2B10 related protein	Cyp2b20	-1.9	Down
Nodal	Ndl	-1.8	Down
Protein tyrosine phosphatase, non-receptor type 16	Ptpn16	-1.8	Down
Cytochrome P450, 39a1 (oxysterol 7alpha-hydroxylase)	Cyp39a1	-1.8	Down
Bicaudal D homolog 2	Bicd2	-1.7	Down
Beta catenin	Catnb	-1.7	Down
A disintegrin and metalloproteinase domain 15	Adam15	-1.6	Down
Notch gene homolog 4	Notch4	-1.5	Down
Protein tyrosine phosphatase, non-receptor type 21	Ptpn21	-1.5	Down
Yes-associated protein	Yap	-1.4	Down

Table 3. Selected Cell Cycle Related and Growth Related Genes at Day 2 after PHx in GPC3 TG Mice Compared with their WT Littermates.

Gene Name	Gene Symbol	Fold Change	
Runt related transcription factor 3	*Runx3*	**8.0**	**Up**
Insulin-like growth factor binding protein 1	*Igfbp1*	**5.1**	**Up**
Growth arrest and DNA-damage-inducible 45 beta	*Gadd45b*	**3.9**	**Up**
Insulin-like growth factor 2, binding protein 3	*Igf2bp3*	**2.6**	**Up**
Fibroblast growth factor 14	*Fgf14*	**2.0**	**Up**
Neural-restrictive silencer factor nrsfrest	*Nrsfrest*	**1.9**	**Up**
Insulin-like growth factor binding protein 3	*Igfbp3*	**1.9**	**Up**
Fibroblast growth factor (acidic) intracellular binding protein	*Fibp*	**1.7**	**Up**
Transforming growth factor beta type I	*Tgfb1*	**1.6**	**Up**
Cyclin-dependent kinase 6	*Cdk6*	**1.6**	**Up**
Histone 4	*Hist4*	**1.6**	**Up**
Fibroblast growth factor receptor 1	*Fgfr1*	**1.6**	**Up**
Cyclin E1	*Ccne1*	1.4	
Cyclin G2	*Ccng2*	1.4	
Insulin-like growth factor 2 receptor	*Igf2r*	1.4	
Cyclin C	*Ccnc*	1.4	
Insulin-like growth factor I receptor	*Igf1r*	1.4	
Cyclin T1	*Ccnt1*	1.4	
Fibroblast growth factor 21	*Fgf21*	1.3	
Fibroblast growth factor 6	*Fgf6*	1.2	

Growth factor receptor bound protein 2-associated protein 1	*Gab1*	1.2	
Cyclin F	*Ccnf*	1.2	
Fibroblast growth factor receptor 4 splice variant 17a	*Fgfr4*	1.2	
Growth arrest and DNA-damage-inducible 45 gamma	*Gadd45g*	1.2	
Cyclin B	*Ccnb*	1.2	
Helicase (DNA) B	*Helb*	1.2	
Heparin-binding EGF-like growth factor precursor	*Hegfl*	1.2	
Cyclin-dependent kinase 9	*Cdk9*	1.2	
Cyclin D3	*Ccnd3*	1.1	
Yes-associated protein	*Yap*	1.1	
Cyclin-dependent kinase 5	*Cdk5*	1.1	
Cyclin D2	*Ccnd2*	1.1	
Jun-B oncogene	*Junb*	1.1	
Catenin beta	*Catnb*	1.1	
Transforming growth factor-alpha	*Tgfa*	1.1	
Cyclin A1	*Ccna1*	**-7.6**	**Down**
Insulin-like growth factor 2	*Igf2*	**-6.3**	**Down**
Cyclin M1	*Ccnm1*	**-5.4**	**Down**
D site albumin promoter binding protein	*Dbp*	**-3.0**	**Down**
Insulin-like growth factor binding protein 4	*Igfbp4*	**-2.4**	**Down**
Insulin-like growth factor binding protein 5	*Igfbp5*	**-2.1**	**Down**
Cyclin-dependent kinase 3	*Cdk3*	**-2.1**	**Down**

Fos-like antigen 1	*Fosl1*	**-2.0**	**Down**
Suc1-associated neurotrophic factor target 2	*Snt2*	**-1.9**	**Down**
Cyclin-dependent kinase inhibitor 1A	*P21*	**-1.8**	**Down**
Fibroblast growth factor 17	*Fgf17*	**-1.7**	**Down**
Growth arrest specific 1	*Gas1*	**-1.7**	**Down**
Transforming growth factor, beta 2	*Tgfb2*	**-1.7**	**Down**
Cyclin E2	*Ccne2*	**-1.7**	**Down**
Insulin-like growth factor binding protein 4	*Igfbp4*	**-1.7**	**Down**
Glypican 6	*Gpc6*	**-1.6**	**Down**
Insulin-like growth factor binding protein 7	*Igfbp7*	**-1.5**	**Down**
Glypican 1	*Gpc1*	**-1.5**	**Down**
CD81 antigen	*Cd81*	**-1.5**	**Down**
Syndecan4	*Sdc4*	-1.4	
Cyclin D1	*Ccnd1*	-1.4	
Kallikrein 13	*Klk13*	-1.4	
Cyclin G	*Ccng*	-1.4	
Insulin-like growth factor binding protein 2	*Igfbp2*	-1.4	
Cyclin A2	*Ccna2*	-1.4	
Growth arrest specific 5	*Gas5*	-1.4	
Nodal	*Ndl*	-1.3	
Insulin-like growth factor binding protein 5	*Igfbp5*	-1.3	
Cyclin M2	*Ccnm2*	-1.3	
FBJ osteosarcoma oncogene	*Fosb*	-1.3	

Cyclin-dependent kinase inhibitor 2A	*Cdkn2a*	-1.2
Cyclin-dependent kinase 2	*Cdk2*	-1.2
Insulin-like growth factor 2, binding protein 3	*Igf2bp3*	-1.2
Cyclin-dependent kinase 12	*Cdk12*	-1.2
Cyclin-dependent kinase 4	*Cdk4*	-1.2
Epidermal growth factor receptor	*Egfr*	-1.2
Cyclin H	*Ccnh*	-1.2
Fibroblast growth factor 1	*Fgf1*	-1.2
Early growth response 1	*Egr1*	-1.1
Cyclin M3	*Ccnm3*	-1.1
Glypican 4	*Gpc4*	-1.1
Epidermal growth factor	*Egf*	-1.1
Insulin-like growth factor 1	*Igf1*	-1.1

BIBLIOGRAPHY

1. Fransson LA. Glypicans. International Journal of Biochemistry & Cell Biology 2003;35:125-129.

2. Song HH, Filmus J. The role of glypicans in mammalian development. Biochimica et Biophysica Acta 2002;1573:241-246.

3. De Cat B, David G. Developmental roles of the glypicans. Seminars in Cell & Developmental Biology 2001;12:117-125.

4. Veugelers M, De Cat B, Ceulemans H, Bruystens AM, Coomans C, Durr J, Vermeesch J, et al. Glypican-6, a new member of the glypican family of cell surface heparan sulfate proteoglycans. J Biol Chem 1999;274:26968-26977.

5. Chen RL, Lander AD. Mechanisms underlying preferential assembly of heparan sulfate on glypican-1. J Biol Chem 2001;276:7507-7517.

6. Filmus J, Selleck SB. Glypicans: proteoglycans with a surprise. J Clin Invest 2001;108:497-501.

7. Filmus J. Glypicans in growth control and cancer. Glycobiology 2001;11:19R-23R.

8. Rapraeger AC. Syndecan-regulated receptor signaling. J Cell Biol 2000;149:995-998.

9. Huber R, Crisponi L, Mazzarella R, Chen CN, Su Y, Shizuya H, Chen EY, et al. Analysis of exon/intron structure and 400 kb of genomic sequence surrounding the 5'-promoter and 3'-terminal ends of the human glypican 3 (GPC3) gene. Genomics 1997;45:48-58.

10. Shen T, Sonoda G, Hamid J, Li M, Filmus J, Buick RN, Testa JR. Mapping of the Simpson-Golabi-Behmel overgrowth syndrome gene (GPC3) to chromosome X in human and rat by fluorescence in situ hybridization. Mamm Genome 1997;8:72.

11. Pilia G, Hughes-Benzie RM, MacKenzie A, Baybayan P, Chen EY, Huber R, Neri G, et al. Mutations in GPC3, a glypican gene, cause the Simpson-Golabi-Behmel overgrowth syndrome. Nat Genet 1996;12:241-247.

12. Pellegrini M, Pilia G, Pantano S, Lucchini F, Uda M, Fumi M, Cao A, et al. Gpc3 expression correlates with the phenotype of the Simpson-Golabi-Behmel syndrome. Dev Dyn 1998;213:431-439.

13. Iglesias BV, Centeno G, Pascuccelli H, Ward F, Peters MG, Filmus J, Puricelli L, et al. Expression pattern of glypican-3 (GPC3) during human embryonic and fetal development. Histol Histopathol 2008;23:1333-1340.

14. Hughes-Benzie RM, Pilia G, Xuan JY, Hunter AG, Chen E, Golabi M, Hurst JA, et al. Simpson-Golabi-Behmel syndrome: genotype/phenotype analysis of 18 affected males from 7 unrelated families. Am J Med Genet 1996;66:227-234.

15. Rodriguez-Criado G, Magano L, Segovia M, Gurrieri F, Neri G, Gonzalez-Meneses A, Gomez de Terreros I, et al. Clinical and molecular studies on two further families with Simpson-Golabi-Behmel syndrome. Am J Med Genet A 2005;138A:272-277.

16. Cano-Gauci DF, Song HH, Yang H, McKerlie C, Choo B, Shi W, Pullano R, et al. Glypican-3-deficient mice exhibit developmental overgrowth and some of the abnormalities typical of Simpson-Golabi-Behmel syndrome. J Cell Biol 1999;146:255-264.

17. Nakatsura T, Kageshita T, Ito S, Wakamatsu K, Monji M, Ikuta Y, Senju S, et al. Identification of glypican-3 as a novel tumor marker for melanoma. Clinical Cancer Research 2004;10:6612-6621.

18. Luo JH, Ren B, Keryanov S, Tseng GC, Rao UN, Monga SP, Strom S, et al. Transcriptomic and genomic analysis of human hepatocellular carcinomas and hepatoblastomas. Hepatology 2006;44:1012-1024.

19. Filmus J, Capurro M. Glypican-3 and alphafetoprotein as diagnostic tests for hepatocellular carcinoma. Molecular Diagnosis 2004;8:207-212.

20. Yamauchi N, Watanabe A, Hishinuma M, Ohashi K, Midorikawa Y, Morishita Y, Niki T, et al. The glypican 3 oncofetal protein is a promising diagnostic marker for hepatocellular carcinoma. Modern Pathology 2005;18:1591-1598.

21. Farooq M, Hwang SY, Park MK, Kim JC, Kim MK, Sung YK. Blocking endogenous glypican-3 expression releases Hep 3B cells from G1 arrest. Molecules & Cells 2003;15:356-360.

22. Ikuta Y, Nakatsura T, Kageshita T, Fukushima S, Ito S, Wakamatsu K, Baba H, et al. Highly sensitive detection of melanoma at an early stage based on the increased serum secreted protein acidic and rich in cysteine and glypican-3 levels. Clin Cancer Res 2005;11:8079-8088.

23. Peters MG, Farias E, Colombo L, Filmus J, Puricelli L, Bal de Kier Joffe E. Inhibition of invasion and metastasis by glypican-3 in a syngeneic breast cancer model. Breast Cancer Res Treat 2003;80:221-232.

24. Kim H, Xu GL, Borczuk AC, Busch S, Filmus J, Capurro M, Brody JS, et al. The heparan sulfate proteoglycan GPC3 is a potential lung tumor suppressor. Am J Respir Cell Mol Biol 2003;29:694-701.

25. Lin H, Huber R, Schlessinger D, Morin PJ. Frequent silencing of the GPC3 gene in ovarian cancer cell lines. Cancer Res 1999;59:807-810.

26. Man XB, Tang L, Zhang BH, Li SJ, Qiu XH, Wu MC, Wang HY. Upregulation of Glypican-3 expression in hepatocellular carcinoma but downregulation in cholangiocarcinoma indicates its differential diagnosis value in primary liver cancers. Liver Int 2005;25:962-966.

27. Murthy SS, Shen T, De Rienzo A, Lee WC, Ferriola PC, Jhanwar SC, Mossman BT, et al. Expression of GPC3, an X-linked recessive overgrowth gene, is silenced in malignant mesothelioma. Oncogene 2000;19:410-416.

28. Xiang YY, Ladeda V, Filmus J. Glypican-3 expression is silenced in human breast cancer. Oncogene 2001;20:7408-7412.

29. Baumhoer D, Tornillo L, Stadlmann S, Roncalli M, Diamantis EK, Terracciano LM. Glypican 3 expression in human nonneoplastic, preneoplastic, and neoplastic tissues: a tissue microarray analysis of 4,387 tissue samples. Am J Clin Pathol 2008;129:899-906.

30. Filmus J, Capurro M. The role of glypican-3 in the regulation of body size and cancer. Cell Cycle 2008;7:2787-2790.

31. Brown DA, Rose JK. Sorting of GPI-anchored proteins to glycolipid-enriched membrane subdomains during transport to the apical cell surface. Cell 1992;68:533-544.

32. Helms JB, Zurzolo C. Lipids as targeting signals: lipid rafts and intracellular trafficking. Traffic 2004;5:247-254.

33. Simons K, Ikonen E. Functional rafts in cell membranes. Nature 1997;387:569-572.

34. Kato M, Wang H, Kainulainen V, Fitzgerald ML, Ledbetter S, Ornitz DM, Bernfield M. Physiological degradation converts the soluble syndecan-1 ectodomain from an inhibitor to a potent activator of FGF-2. Nat Med 1998;4:691-697.

35. Fransson LA, Belting M, Edgren G, Jonsson M, Mani K, Schmidtchen A, Wiik P. Degradation and reprocessing of heparan sulphate in recycling glypican (heparan sulphate proteoglycan). Trends in Glycoscience and Glycotechnology 1998;10:81-94.

36. Anderson RG, Kamen BA, Rothberg KG, Lacey SW. Potocytosis: sequestration and transport of small molecules by caveolae. Science 1992;255:410-411.

37. Grisaru S, Cano-Gauci D, Tee J, Filmus J, Rosenblum ND. Glypican-3 modulates BMP- and FGF-mediated effects during renal branching morphogenesis. Dev Biol 2001;231:31-46.

38. Midorikawa Y, Ishikawa S, Iwanari H, Imamura T, Sakamoto H, Miyazono K, Kodama T, et al. Glypican-3, overexpressed in hepatocellular carcinoma, modulates FGF2 and BMP-7 signaling. Int J Cancer 2003;103:455-465.

39. Song HH, Shi W, Xiang YY, Filmus J. The loss of glypican-3 induces alterations in Wnt signaling. J Biol Chem 2005;280:2116-2125.

40. Stigliano I, Puricelli L, Filmus J, Sogayar MC, Bal de Kier Joffe E, Peters MG. Glypican-3 regulates migration, adhesion and actin cytoskeleton organization in mammary tumor cells through Wnt signaling modulation. Breast Cancer Res Treat 2009;114:251-262.

41. Gonzalez AD, Kaya M, Shi W, Song H, Testa JR, Penn LZ, Filmus J. OCI-5/GPC3, a glypican encoded by a gene that is mutated in the Simpson-Golabi-Behmel overgrowth syndrome, induces apoptosis in a cell line-specific manner. J Cell Biol 1998;141:1407-1414.

42. Watanabe K, Yamada H, Yamaguchi Y. K-glypican: a novel GPI-anchored heparan sulfate proteoglycan that is highly expressed in developing brain and kidney. J Cell Biol 1995;130:1207-1218.

43. Capurro M, Shi W, Sandal S, Filmus J. Processing by Convertases Is Not Required for Glypican-3-induced Stimulation of Hepatocellular Carcinoma Growth. J Biol Chem 2005;280:41201-41206.

44. Yayon A, Klagsbrun M, Esko JD, Leder P, Ornitz DM. Cell surface, heparin-like molecules are required for binding of basic fibroblast growth factor to its high affinity receptor. Cell 1991;64:841-848.

45. Steinfeld R, Van Den Berghe H, David G. Stimulation of fibroblast growth factor receptor-1 occupancy and signaling by cell surface-associated syndecans and glypican. J Cell Biol 1996;133:405-416.

46. Piscione TD, Phan T, Rosenblum ND. BMP7 controls collecting tubule cell proliferation and apoptosis via Smad1-dependent and -independent pathways. Am J Physiol Renal Physiol 2001;280:F19-33.

47. Capurro MI, Xiang YY, Lobe C, Filmus J. Glypican-3 promotes the growth of hepatocellular carcinoma by stimulating canonical Wnt signaling. Cancer Res 2005;65:6245-6254.

48. Zeng G, Awan F, Otruba W, Muller P, Apte U, Tan X, Gandhi C, et al. Wnt'er in liver: expression of Wnt and frizzled genes in mouse. Hepatology 2007;45:195-204.

49. Capurro MI, Shi W, Sandal S, Filmus J. Processing by convertases is not required for glypican-3-induced stimulation of hepatocellular carcinoma growth. J Biol Chem 2005;280:41201-41206.

50. Zittermann SI, Capurro MI, Shi W, Filmus J. Soluble glypican 3 inhibits the growth of hepatocellular carcinoma in vitro and in vivo. Int J Cancer 2010;126:1291-1301.

51. Song HH, Shi W, Filmus J. OCI-5/rat glypican-3 binds to fibroblast growth factor-2 but not to insulin-like growth factor-2. J Biol Chem 1997;272:7574-7577.

52. Morford LA, Davis C, Jin L, Dobierzewska A, Peterson ML, Spear BT. The oncofetal gene glypican 3 is regulated in the postnatal liver by zinc fingers and homeoboxes 2 and in the regenerating liver by alpha-fetoprotein regulator 2. Hepatology 2007;46:1541-1547.

53. Belayew A, Tilghman SM. Genetic analysis of alpha-fetoprotein synthesis in mice. Mol Cell Biol 1982;2:1427-1435.

54. Spear BT. Alpha-fetoprotein gene regulation: lessons from transgenic mice. Semin Cancer Biol 1999;9:109-116.

55. Baig JA, Alam JM, Mahmood SR, Baig M, Shaheen R, Sultana I, Waheed A. Hepatocellular carcinoma (HCC) and diagnostic significance of A-fetoprotein (AFP). J Ayub Med Coll Abbottabad 2009;21:72-75.

56. Okuda N, Nakao A, Takeda S, Oshima K, Kanazumi N, Nonami T, Kurokawa T, et al. Clinical significance of alpha-fetoprotein mRNA during perioperative period in HCC. Hepatogastroenterology 1999;46:381-386.

57. Llovet JM, Chen Y, Wurmbach E, Roayaie S, Fiel MI, Schwartz M, Thung SN, et al. A molecular signature to discriminate dysplastic nodules from early hepatocellular carcinoma in HCV cirrhosis. Gastroenterology 2006;131:1758-1767.

58. Wang XY, Degos F, Dubois S, Tessiore S, Allegretta M, Guttmann RD, Jothy S, et al. Glypican-3 expression in hepatocellular tumors: diagnostic value for preneoplastic lesions and hepatocellular carcinomas. Hum Pathol 2006;37:1435-1441.

59. Pachnis V, Brannan CI, Tilghman SM. The structure and expression of a novel gene activated in early mouse embryogenesis. Embo J 1988;7:673-681.

60. Lai JP, Sandhu DS, Yu C, Han T, Moser CD, Jackson KK, Guerrero RB, et al. Sulfatase 2 up-regulates glypican 3, promotes fibroblast growth factor signaling, and decreases survival in hepatocellular carcinoma. Hepatology 2008;47:1211-1222.

61. Monk M. Methylation and the X chromosome. Bioessays 1986;4:204-208.

62. Boily G, Saikali Z, Sinnett D. Methylation analysis of the glypican 3 gene in embryonal tumours. Br J Cancer 2004;90:1606-1611.

63. Huber R, Hansen RS, Strazzullo M, Pengue G, Mazzarella R, D'Urso M, Schlessinger D, et al. DNA methylation in transcriptional repression of two differentially expressed X-linked genes, GPC3 and SYBL1. Proc Natl Acad Sci U S A 1999;96:616-621.

64. Kanel G, Korula J. Atlas of Liver Pathology. 2005.

65. Dietschy JM. Regulation of cholesterol metabolism in man and in other species. Klin Wochenschr 1984;62:338-345.

66. Ling WH, Jones PJ. Dietary phytosterols: a review of metabolism, benefits and side effects. Life Sci 1995;57:195-206.

67. Cunningham CC, Van Horn CG. Energy availability and alcohol-related liver pathology. Alcohol Res Health 2003;27:291-299.

68. Michalopoulos GK. Liver regeneration. Journal of Cellular Physiology 2007;213:286-300.

69. Michalopoulos GK, DeFrances MC. Liver regeneration. Science 1997;276:60-66.

70. Higgins G, Anderson R. Experimental pathology of liver: restoration of liver of the white rat following partial surgical removal. Arch Pathol 1931;12:186-202.

71. Mitchell C, Willenbring H. A reproducible and well-tolerated method for 2/3 partial hepatectomy in mice. Nat Protoc 2008;3:1167-1170.

72. Rabes HM. Kinetics of hepatocellular proliferation as a function of the microvascular structure and functional state of the liver. Ciba Found Symp 1977:31-53.

73. Michalopoulos GK, Bowen WC, Zajac VF, Beer-Stolz D, Watkins S, Kostrubsky V, Strom SC. Morphogenetic events in mixed cultures of rat hepatocytes and nonparenchymal cells maintained in biological matrices in the presence of hepatocyte growth factor and epidermal growth factor.[see comment]. Hepatology 1999;29:90-100.

74. Taub R. Liver regeneration: from myth to mechanism. Nat Rev Mol Cell Biol 2004;5:836-847.

75. Swindle CS, Tran KT, Johnson TD, Banerjee P, Mayes AM, Griffith L, Wells A. Epidermal growth factor (EGF)-like repeats of human tenascin-C as ligands for EGF receptor. J Cell Biol 2001;154:459-468.

76. Mars WM, Liu ML, Kitson RP, Goldfarb RH, Gabauer MK, Michalopoulos GK. Immediate early detection of urokinase receptor after partial hepatectomy and its implications for initiation of liver regeneration. Hepatology 1995;21:1695-1701.

77. Kim TH, Mars WM, Stolz DB, Petersen BE, Michalopoulos GK. Extracellular matrix remodeling at the early stages of liver regeneration in the rat. Hepatology 1997;26:896-904.

78. Mars WM, Zarnegar R, Michalopoulos GK. Activation of hepatocyte growth factor by the plasminogen activators uPA and tPA. Am J Pathol 1993;143:949-958.

79. Stolz DB, Mars WM, Petersen BE, Kim TH, Michalopoulos GK. Growth factor signal transduction immediately after two-thirds partial hepatectomy in the rat. Cancer Res 1999;59:3954-3960.

80. Cressman DE, Diamond RH, Taub R. Rapid activation of the Stat3 transcription complex in liver regeneration. Hepatology 1995;21:1443-1449.

81. Monga SP, Pediaditakis P, Mule K, Stolz DB, Michalopoulos GK. Changes in WNT/beta-catenin pathway during regulated growth in rat liver regeneration. Hepatology 2001;33:1098-1109.

82. Kohler C, Bell AW, Bowen WC, Monga SP, Fleig W, Michalopoulos GK. Expression of Notch-1 and its ligand Jagged-1 in rat liver during liver regeneration. Hepatology 2004;39:1056-1065.

83. Hsu JC, Bravo R, Taub R. Interactions among LRF-1, JunB, c-Jun, and c-Fos define a regulatory program in the G1 phase of liver regeneration. Mol Cell Biol 1992;12:4654-4665.

84. Kato A, Ota S, Bamba H, Wong RM, Ohmura E, Imai Y, Matsuzaki F. Regulation of cyclin D-dependent kinase activity in rat liver regeneration. Biochem Biophys Res Commun 1998;245:70-74.

85. Friedman JR, Larris B, Le PP, Peiris TH, Arsenlis A, Schug J, Tobias JW, et al. Orthogonal analysis of C/EBPbeta targets in vivo during liver proliferation. Proc Natl Acad Sci U S A 2004;101:12986-12991.

86. Martinez-Hernandez A, Amenta PS. The extracellular matrix in hepatic regeneration. Faseb J 1995;9:1401-1410.

87. Sakamoto T, Liu Z, Murase N, Ezure T, Yokomuro S, Poli V, Demetris AJ. Mitosis and apoptosis in the liver of interleukin-6-deficient mice after partial hepatectomy. Hepatology 1999;29:403-411.

88. Wagenaar GT, Chamuleau RA, Pool CW, de Haan JG, Maas MA, Korfage HA, Lamers WH. Distribution and activity of glutamine synthase and carbamoylphosphate synthase upon enlargement of the liver lobule by repeated partial hepatectomies. J Hepatol 1993;17:397-407.

89. Gkretsi V, Bowen WC, Yang Y, Wu C, Michalopoulos GK. Integrin-linked kinase is involved in matrix-induced hepatocyte differentiation. Biochem Biophys Res Commun 2007;353:638-643.

90. Gallai M, Sebestyen A, Nagy P, Kovalszky I, Onody T, Thorgeirsson SS. Proteoglycan gene expression in rat liver after partial hepatectomy. Biochem Biophys Res Commun 1996;228:690-694.

91. Rudolph KL, Trautwein C, Kubicka S, Rakemann T, Bahr MJ, Sedlaczek N, Schuppan D, et al. Differential regulation of extracellular matrix synthesis during liver regeneration after partial hepatectomy in rats. Hepatology 1999;30:1159-1166.

92. Mars WM, Kim TH, Stolz DB, Liu ML, Michalopoulos GK. Presence of urokinase in serum-free primary rat hepatocyte cultures and its role in activating hepatocyte growth factor. Cancer Res 1996;56:2837-2843.

93. Matsuoka M, Pham NT, Tsukamoto H. Differential effects of interleukin-1 alpha, tumor necrosis factor alpha, and transforming growth factor beta 1 on cell proliferation and collagen formation by cultured fat-storing cells. Liver 1989;9:71-78.

94. Block GD, Locker J, Bowen WC, Petersen BE, Katyal S, Strom SC, Riley T, et al. Population expansion, clonal growth, and specific differentiation patterns in primary cultures of hepatocytes induced by HGF/SF, EGF and TGF alpha in a chemically defined (HGM) medium. Journal of Cell Biology 1996;132:1133-1149.

95. Seglen PO. Preparation of isolated rat liver cells. Methods in Cell Biology 1976;13:29-83.

96. Tsuda H, Yamada S, Miyazono H, Morikawa K, Yoshida K, Goto F, Tamura JI, et al. Substrate specificity studies of Flavobacterium chondroitinase C and heparitinases towards the glycosaminoglycan--protein linkage region. Use of a sensitive analytical method developed by chromophore-labeling of linkage glycoserines using dimethylaminoazobenzenesulfonyl chloride. Eur J Biochem 1999;262:127-133.

97. Summerton J. Endo-Porter: a novel reagent for safe, effective delivery of substances into cells. Ann N Y Acad Sci 2005;1058:62-75.

98. Raiborg C, Stenmark H. Hrs and endocytic sorting of ubiquitinated membrane proteins. Cell Structure & Function 2002;27:403-408.

99. Levy S, Todd SC, Maecker HT. CD81 (TAPA-1): a molecule involved in signal transduction and cell adhesion in the immune system. Annual Review of Immunology 1998;16:89-109.

100. Cocquerel L, Kuo CC, Dubuisson J, Levy S. CD81-dependent binding of hepatitis C virus E1E2 heterodimers. J Virol 2003;77:10677-10683.

101. Grozdanov PN, Yovchev MI, Dabeva MD. The oncofetal protein glypican-3 is a novel marker of hepatic progenitor/oval cells. Lab Invest 2006;86:1272-1284.

102. Kleeff J, Ishiwata T, Kumbasar A, Friess H, Buchler MW, Lander AD, Korc M. The cell-surface heparan sulfate proteoglycan glypican-1 regulates growth factor action in pancreatic carcinoma cells and is overexpressed in human pancreatic cancer. J Clin Invest 1998;102:1662-1673.

103. Hogan B, Costantini F, Lacy E. Manipulating the mouse embryo: A Laboratory Manual. . Cold Spring Harbor, NY: Cold Spring Harbor Laboratory, 1986: 174-175.

104. Liu Y, Bell AW, Michalopoulos GK, Zarnegar R. The mouse hepatocyte growth factor-encoding gene: structural organization and evolutionary conservation. Gene 1994;144:179-187.

105. Liu B, Paranjpe S, Bowen WC, Bell AW, Luo JH, Yu YP, Mars WM, et al. Investigation of the role of glypican 3 in liver regeneration and hepatocyte proliferation. Am J Pathol 2009;175:717-724.

106. Ohtsubo K, Nomaguchi TA. A flow cytofluorometric study on age-dependent ploidy class changes in mouse hepatocyte nuclei. Mech Ageing Dev 1986;36:125-131.

107. Shima A, Sugahara T. Age-dependent ploidy class changes in mouse hepatocyte nuclei as revealed by Feulgen-DNA cytofluorometry. Exp Gerontol 1976;11:193-203.

108. Morimoto T, Tsujinaka T, Yano M, Iijima S, Ebisui C, Kan K, Kishibuchi M, et al. Regulation of albumin synthesis after hepatectomy and in the acute inflammation phase of rat liver The Journal of Nutritional Biochemistry 1995;6:522-527.

109. Trautwein C, Rakemann T, Pietrangelo A, Plumpe J, Montosi G, Manns MP. C/EBP-beta/LAP controls down-regulation of albumin gene transcription during liver regeneration. J Biol Chem 1996;271:22262-22270.

110. Morimoto T, Tsujinaka T, Yano M, Ogawa A, Kishibuchi M, Morita S, Shiozaki H, et al. Regulation of albumin mRNA and its promoter-binding nuclear factors under different perioperative nutritional methods in hepatectomized rats. Am J Surg 1998;175:221-225; discussion 225-226.

111. Mueller CR. The down-regulation of albumin transcription during regeneration is due to the loss of HNF-1 and the D-site transcription factors. DNA Cell Biol 1992;11:559-566.

112. Minuk GY, Gauthier T. The effect of gamma-aminobutyric acid on hepatic regenerative activity following partial hepatectomy in rats. Gastroenterology 1993;104:217-221.

113. Gao J, Chen Y, Wu KC, Liu J, Zhao YQ, Pan YL, Du R, et al. RUNX3 directly interacts with intracellular domain of Notch1 and suppresses Notch signaling in hepatocellular carcinoma cells. Exp Cell Res 2010;316:149-157.

114. Skarpen E, Oksvold MP, Grosvik H, Widnes C, Huitfeldt HS. Altered regulation of EGF receptor signaling following a partial hepatectomy. J Cell Physiol 2005;202:707-716.

115. Zhang X, Liu Y. Suppression of HGF receptor gene expression by oxidative stress is mediated through the interplay between Sp1 and Egr-1. Am J Physiol Renal Physiol 2003;284:F1216-1225.

116. Mullany LK, White P, Hanse EA, Nelsen CJ, Goggin MM, Mullany JE, Anttila CK, et al. Distinct proliferative and transcriptional effects of the D-type cyclins in vivo. Cell Cycle 2008;7:2215-2224.

117. Greenbaum LE, Cressman DE, Haber BA, Taub R. Coexistence of C/EBP alpha, beta, growth-induced proteins and DNA synthesis in hepatocytes during liver regeneration. Implications for maintenance of the differentiated state during liver growth. J Clin Invest 1995;96:1351-1365.

118. Song H, Mak KK, Topol L, Yun K, Hu J, Garrett L, Chen Y, et al. Mammalian Mst1 and Mst2 kinases play essential roles in organ size control and tumor suppression. Proc Natl Acad Sci U S A 2010;107:1431-1436.

119. Zhao B, Wei X, Li W, Udan RS, Yang Q, Kim J, Xie J, et al. Inactivation of YAP oncoprotein by the Hippo pathway is involved in cell contact inhibition and tissue growth control. Genes Dev 2007;21:2747-2761.

120. Ikeda H, Nagoshi S, Ohno A, Yanase M, Maekawa H, Fujiwara K. Activated rat stellate cells express c-met and respond to hepatocyte growth factor to enhance transforming growth factor beta1 expression and DNA synthesis. Biochem Biophys Res Commun 1998;250:769-775.

121. Houck KA, Michalopoulos GK. Altered responses of regenerating hepatocytes to norepinephrine and transforming growth factor type beta. J Cell Physiol 1989;141:503-509.

122. Gohda E, Matsunaga T, Kataoka H, Yamamoto I. TGF-beta is a potent inhibitor of hepatocyte growth factor secretion by human fibroblasts. Cell Biol Int Rep 1992;16:917-926.

123. Oe S, Lemmer ER, Conner EA, Factor VM, Leveen P, Larsson J, Karlsson S, et al. Intact signaling by transforming growth factor beta is not required for termination of liver regeneration in mice. Hepatology 2004;40:1098-1105.

124. Levy S, Shoham T. The tetraspanin web modulates immune-signalling complexes. Nat Rev Immunol 2005;5:136-148.

125. Stipp CS, Hemler ME. Transmembrane-4-superfamily proteins CD151 and CD81 associate with alpha 3 beta 1 integrin, and selectively contribute to alpha 3 beta 1-dependent neurite outgrowth. J Cell Sci 2000;113 (Pt 11):1871-1882.

126. Yanez-Mo M, Alfranca A, Cabanas C, Marazuela M, Tejedor R, Ursa MA, Ashman LK, et al. Regulation of endothelial cell motility by complexes of tetraspan molecules CD81/TAPA-1 and CD151/PETA-3 with alpha3 beta1 integrin localized at endothelial lateral junctions. J Cell Biol 1998;141:791-804.

127. Carloni V, Mazzocca A, Ravichandran KS. Tetraspanin CD81 is linked to ERK/MAPKinase signaling by Shc in liver tumor cells. Oncogene 2004;23:1566-1574.

128. Hemler ME. Tetraspanin functions and associated microdomains. Nat Rev Mol Cell Biol 2005;6:801-811.

129. Yunta M, Lazo PA. Tetraspanin proteins as organisers of membrane microdomains and signalling complexes. Cell Signal 2003;15:559-564.

130. Le Naour F, Andre M, Boucheix C, Rubinstein E. Membrane microdomains and proteomics: lessons from tetraspanin microdomains and comparison with lipid rafts. Proteomics 2006;6:6447-6454.

131. Yanez-Mo M, Barreiro O, Gordon-Alonso M, Sala-Valdes M, Sanchez-Madrid F. Tetraspanin-enriched microdomains: a functional unit in cell plasma membranes. Trends Cell Biol 2009;19:434-446.

132. Zoller M. Tetraspanins: push and pull in suppressing and promoting metastasis. Nat Rev Cancer 2009;9:40-55.